

FRAME ANALYSIS OF
THIN SHELLS

By

RONALD A. APANIAN

Bachelor of Science
University of North Dakota
Grand Forks, North Dakota
1956

Master of Science
University of North Dakota
Grand Forks, North Dakota
1958

Submitted to the faculty of the Graduate
College of the Oklahoma State University
in partial fulfillment of the
requirements for the degree of
DOCTOR OF PHILOSOPHY
May, 1967

JAN 9 1968

FRAME ANALYSIS OF
THIN SHELLS

Thesis Approved:

M. Kelly

Thesis Adviser

A. R. Howell

Albert Salama

P. Dranfeld

D. N. Durbin

Dean of the Graduate College

658305

PREFACE

The author wishes to take this opportunity to express his gratitude and sincere appreciation to the following individuals and organizations:

To his committee members Dr. A. F. Gaudy, Dr. M. N. Reddy, Dr. A. E. Salama and Dr. P. Dransfield for their assistance and encouragement;

To faculty members of the Civil Engineering Department for their valuable instruction;

To the staff of the Oklahoma State University Library;

To Dr. D. D. Grosvenor and staff of the Oklahoma State University Computer Center;

To his wife and children for their love and understanding through trying times;

To the University of North Dakota for granting a leave of absence;

To the National Science Foundation for awarding the National Science Foundation Faculty Fellowship;

To Mrs. Carl Estes for her wonderful cooperation and careful typing of the manuscript;

To Mr. Eldon Hardy for preparing the final sketches.

In addition, the author wishes to acknowledge the friendship and inspiration derived from his fellow graduate students, in particular, Mr. Harry Lundgren, Mr. Charles Lindberg and Mr. Johnny Mack Hutt.

R. A. A.

TABLE OF CONTENTS

Chapter	Page
I. INTRODUCTION	1
1.1 Statement of the Problem	1
1.2 Historical Notes	2
II. MATHEMATICAL FORMULATION OF ELEMENT STIFFNESSES	6
2.1 General	6
2.2 Plane Stress Stiffness Matrix.	8
2.3 Bending Stiffness Matrix	22
2.4 Total Element Stiffness Matrix	36
III. FORMULATION AND SOLUTION	39
3.1 Axes Transformation	39
3.2 Structural Stiffness Matrix	42
3.3 Boundary Conditions	43
3.4 Skewed Boundaries	44
3.5 Deformations	46
3.6 Stresses and Stress Resultants	46
IV. APPLICATION TO HYPERBOLIC PARABOLOID SHELLS	48
4.1 General Procedure	48
4.2 Edge Supported Shell	49
4.3 Inverted Umbrella Shell	52
V. SUMMARY AND CONCLUSIONS	60
5.1 Summary.	60
5.2 Discussion of Results	60
5.3 Conclusions and Possible Extensions	63
BIBLIOGRAPHY	64
APPENDIX A. MATRIX $[T_b]$	67
APPENDIX B. COMPUTER ANALYSIS	80

LIST OF TABLES

Table	Page
I. Stress Function for Plane Stress	11
II. Matrix $[H_p]$	13
III. Coefficients for Matrix $[H_p]$	14
IV. Edge Displacement Matrix for Plane Stress .	17
V. Matrix $[R_p]^T$	19
VI. Matrix $[T_p]$	21
VII. Matrix $[P_b]$	26
VIII. Matrix $[H_b]$	28
IX. Coefficients for Matrix $[H_b]$	29
X. Edge Displacement Matrix for Bending	32
XI. Matrix $[R_b]^T$	35
XII. Element Stiffness Matrix	38
XIII. Properties of Edge Supported Shell	50
XIV. Deformations for Edge Supported Shell . . .	54
XV. Properties of Inverted Umbrella Shell . . .	55
XVI. Deformations for Inverted Umbrella Shell . .	59
XVII. Bending Moments for Shell of Figure 14 . . .	62

LIST OF ILLUSTRATIONS

Figure	Page
1. Element Geometry	9
2. In-Plane Stresses and Stress Resultants . . .	9
3. Generalized Nodal Displacements for Plane Stress	16
4. Edge Displacements for Plane Stress	16
5. Edge Forces for Plane Stress	18
6. Bending Stress Distribution	23
7. Bending Stress Resultants	25
8. General Displacements	30
9. Boundary Displacements Due to Bending	31
10. Generalized Nodal Displacements Due to Bending	33
11. Edge Actions Due to Bending	33
12. Axes Reference Systems	39
13. Skewed Boundary Axes	44
14. Edge Supported Shell	50
15. Finite Element Idealization of Edge Supported Shell	51
16. Vertical Deflections for Edge Supported Shell	53
17. Inverted Umbrella Shell	55
18. Ribs and Edge Beams for Inverted Umbrella Shell	58

Figure	Page
19. Finite Element Idealization of Inverted Umbrella Shell	57
20. Vertical Deflections for Inverted Umbrella Shell	58
21. Vertical Deflection Profile Along Y-Axis of Edge Supported Shell	61

NOMENCLATURE

a, b, c, d, f, g	Geometry of triangular element.
a — superscript	Indicates quantity in elemental system.
b — superscript	Indicates quantity in skewed system.
b — subscript	Quantity refers to bending action.
E	Modulus of elasticity.
F	External loads.
i, j, k	Node points of finite element.
K	Stiffness matrix.
M_x, M_y, M_z, M_{xy}	Moment stress resultants.
N_x, N_y, N_{xy}	Force stress resultants.
n	Number of nodes.
o — superscript	Indicates quantity in structural system.
p — subscript	Quantity refers to plane stress.
Q_{zx}, Q_{zy}	Force stress resultants.
q	Generalized nodal displacements.
r	Number of boundary restraints.
S	Actions.
SK	Structural stiffness matrix.
t	Thickness.
\bar{U}	Internal strain energy.
U, V	In-plane node displacements.
u, v	In-plane displacements.

\bar{W}	Work of edge forces.
W	Normal bending displacement.
x, y, z	System of axes.
\bar{Z}, Z'	Multipliers of bending stress function.
α, β, γ	Direction cosines.
α_m, β_m	Parameters in stress function.
$\gamma_{xy}, \gamma_{zx}, \gamma_{zy}$	Strain components.
$\epsilon_x, \epsilon_y, \epsilon_{xy}$	Strain components.
η	Coordinate.
θ	Rotational displacement.
λ	Coordinate.
ν	Poisson's ratio.
$\bar{\nu}$	$(1 + 2\nu)$.
ξ	Coordinate.
π	Complementary energy.
$\sigma_x, \sigma_y, \sigma_{xy}, \sigma_{zx}, \sigma_{zy}$	Stress components.
Ψ	Transformation matrix.
Ω	Transformation matrix.
ω	Angle of skewed boundary.
$[\]$	Square or rectangular matrix.
$[\]$	Row matrix.
$\{ \}$	Column matrix.
$[\]^{-1}$	Matrix inverse.
$[\]^T$	Matrix transpose.

CHAPTER I

INTRODUCTION

1.1 Statement of the Problem

The analysis of shells of double curvature, in particular hyperbolic paraboloidal shells, is investigated. Both membrane and bending deformations are considered. The continuous shell is discretized by a number of triangular shaped plane finite elements which are connected together only at their node points. Continuity of deformations is maintained across the boundary lines separating the elements. Equilibrium is established within the element and at the node points. The element properties are determined and combined to define the elastic characteristics of the total shell and deformations corresponding to a particular set of load and boundary conditions are determined. The critical phase of the analysis is the evaluation of the elastic characteristics, expressed in stiffness matrix form, of the individual finite elements and it is with this phase that a major portion of this investigation is concerned.

Material of the shell is assumed to be continuous, homogenous and isotropic. Shell thickness is considered to be small in comparison with other dimensions and the well

known assumptions of small deflection theory are employed.

For the purpose of this study, the problem is considered solved when the structural stiffness matrix is derived and deformations of the shell are determined.

1.2 Historical Notes

In recent years thin shells of double curvature have been frequently used in construction, especially for roof systems. The hyperbolic paraboloid is one of the most popular of the doubly-curved surfaces and has received considerable attention in the past decade. Felix Candella (1) has summarized the many advantages of the hyperbolic paraboloid in one of his numerous contributions to the field of shell construction. One of the advantages he lists is the simplicity of the differential equation which governs the state of stress in the shell provided that the shell acts as a membrane.

The potentialities of this doubly-curved surface were first exploited by Aïmond (2) in the early 1930's. Since that time an extensive amount of literature on the subject has been published. However, it has been restricted almost entirely to the membrane, or momentless, stress condition.

Past experience with structures designed by the membrane theory has shown that they perform satisfactorily when subjected to loads that are uniformly distributed without abrupt changes in intensity. For other load conditions however, the membrane theory is inadequate and does not

yield realistic results. There are also a number of support conditions for which the membrane theory yields unsatisfactory solutions. In these cases the effects of bending action must be included in the analysis and design.

Although a complete general theory of shells of arbitrary shape has been formulated, its application to the hyperbolic paraboloid is mathematically complex (3). The complexity of this formulation is greatly reduced by introducing the concept of shallow shells, however, the solution remains difficult. An equivalent shallow shell theory has been given by Margurre (4), while perhaps the most exact existing theory of hyperbolic paraboloids bounded by a rectangular set of characteristics is due to Bongard (5).

A recent paper by Chetty and Tottenham (6) investigates the linear bending analysis of the stresses and deformations of a thin shallow rectangular hyperbolic paraboloid shell subjected to uniform normal pressure. The authors discuss and compare the Vlasov and Bongard governing equations.

The idea of representing a continuous elastic medium by discrete finite elements is by no means new. Hrennikoff (7) used a system of elastic bars to represent a flat plate structure as early as 1941. In the late 1940's and early 1950's several investigators reported contributions in connection with wing deflections and other aircraft related structures by using plate assemblages and influence coefficients (8, 9, 10).

One of the first significant contributions on finite

elements, as such, was presented by Turner, Clough, Martin and Topp (11). They derived a stiffness matrix in implicit form for a triangular and a rectangular element subjected to a plane stress condition. The solution was based on an assumed displacement function over the element.

Clough (12) presented a paper dealing with finite elements in plane stress. He also derived the element stiffness matrix on the basis of an assumed displacement function. In 1961, Melosh (13) contributed a paper concerned with the analysis of thin plates in bending. An assumed displacement function was used to derive the element stiffness matrix. A second paper by Melosh (14) listed what he termed requirements that must be satisfied by an assumed displacement function.

Zienkiewicz and Cheung (15, 16, 17) have contributed a number of papers to the rapidly growing list of literature related to the use of finite elements in structural analysis. They discussed the successful use of finite elements in the analysis of flat plates and arch dams.

Rectangular elements have been shown to yield accurate displacement results for plate structures and shell structures of single curvature. Results obtained with the use of triangular elements for the same structures have proved to be somewhat less accurate. The inaccuracies appear to be due to the lack of compatibility of deformations along common sides of adjacent elements. Using an assumed displacement function for a rectangular element, compatibility

of vertical displacement and slope tangential to the boundary can be maintained, however, compatibility of slope normal to the boundary is violated. For other shaped elements even the vertical displacements are discontinuous. This appears to have a very significant influence on triangular elements. Because of this, rectangular elements have been used much more frequently than elements of other geometric shape.

Certain types of structures, irregular shaped plates, plates with openings, doubly-curved shells, et cetera, cannot be discretized by rectangular elements and thus it is necessary to use some other geometric shape. The above mentioned disadvantage of the triangular element can be eliminated, or reduced, by using an assumed stress function, rather than displacement function, as the basis for derivation of the element stiffnesses. Such a procedure is discussed by Pian (18) for a plane stress condition. Severn and Taylor (19) use an assumed stress function for solving plate bending problems.

CHAPTER II

MATHEMATICAL FORMULATION OF ELEMENT STIFFNESSES

2.1 General

A major criticism of triangular elements used for forming the model of a two-dimensional structure is that the resulting accuracy is not as good as that obtained with rectangular elements. Such results have been reported by a number of investigators when using a displacement function to calculate the element stiffnesses (20). The basic reason for this is that the assumed displacement patterns do not satisfy conditions of compatibility across the edges separating the elements. When a cubic displacement function is assumed for a rectangular element, the displacement along any edge may be described by a cubic equation. The form of this cubic equation may be specified by four constants, two slopes and two vertical displacements at the node points which the edge connects. Thus, the vertical displacement along any edge is expressed in terms of only two nodes and continuity is maintained. However, two slopes, one at each node, are not sufficient to determine the three constants in the quadratic slope displacement function. Thus, in general, compatibility of normal slopes at the edges of two

adjacent elements is violated. For geometrical shapes other than the rectangle, the cubic equation for vertical displacement along an edge involves node points not necessarily on that edge and, therefore, vertical displacements are also discontinuous. This incompatibility has a pronounced effect on solutions involving triangular elements.

Compatibility of vertical displacements and slopes along the edges of two adjacent elements can be forced by a procedure discussed by Severn and Taylor (19) and used in this paper. The element stiffness matrix is derived on the basis of an assumed stress distribution rather than a displacement function by applying the principle of minimum complementary energy. Details for a plane stress condition and bending are presented in the following sections of this chapter. The two important quantities to be determined are the strain energy stored in the element and the work performed by equivalent edge forces acting through the edge displacements. Geometry of the triangular element is shown in Figure 1.

The steps in the mathematical procedure for deriving the element stiffness matrix are listed below.

- a) Stress functions.
- b) Stress resultants.
- c) Equilibrium.
- d) Stress-strain relationship.
- e) Strain energy.
- f) Boundary displacements.

- g) Edge forces.
- h) Work of edge forces.
- i) Complementary energy.
- j) Element stiffness matrix.

The steps are carried out for a plane stress condition in section 2.2 and for bending in section 2.3.

2.2 Plane Stress Stiffness Matrix

a) Stress functions—For any point in the triangular element of Figure 1 it is assumed that the three stress components may be expressed as a function of the coordinates of the point and a set of parameters, α_m . The three stresses are assumed to be of constant magnitude across the depth of the element while varying parabolically in the plane of the element. An infinitesimal element is isolated and shown in Figure 2a. The assumed stress equations are:

$$\sigma_x = \alpha_1 + \alpha_2 \bar{x} + \alpha_3 \bar{y}^2 + \alpha_4 \bar{x}^2 + \alpha_5 \bar{x}\bar{y} + \alpha_6 \bar{y}^2 \quad (1a)$$

$$\sigma_y = \alpha_7 + \alpha_8 \bar{x} + \alpha_9 \bar{y} + \alpha_{10} \bar{x}^2 + \alpha_{11} \bar{x}\bar{y} + \alpha_{12} \bar{y}^2 \quad (1b)$$

$$\sigma_{xy} = \alpha_{13} + \alpha_{14} \bar{x} + \alpha_{15} \bar{y} + \alpha_{16} \bar{x}^2 + \alpha_{17} \bar{x}\bar{y} + \alpha_{18} \bar{y}^2 \quad (1c)$$

where

$$\bar{x} = \frac{x}{a} \quad \bar{y} = \frac{y}{b}.$$

b) Stress resultants—Stress resultants per unit length are calculated by integrating equations (1) over the depth of the element and are shown in Figure 2b. They are expressed as:

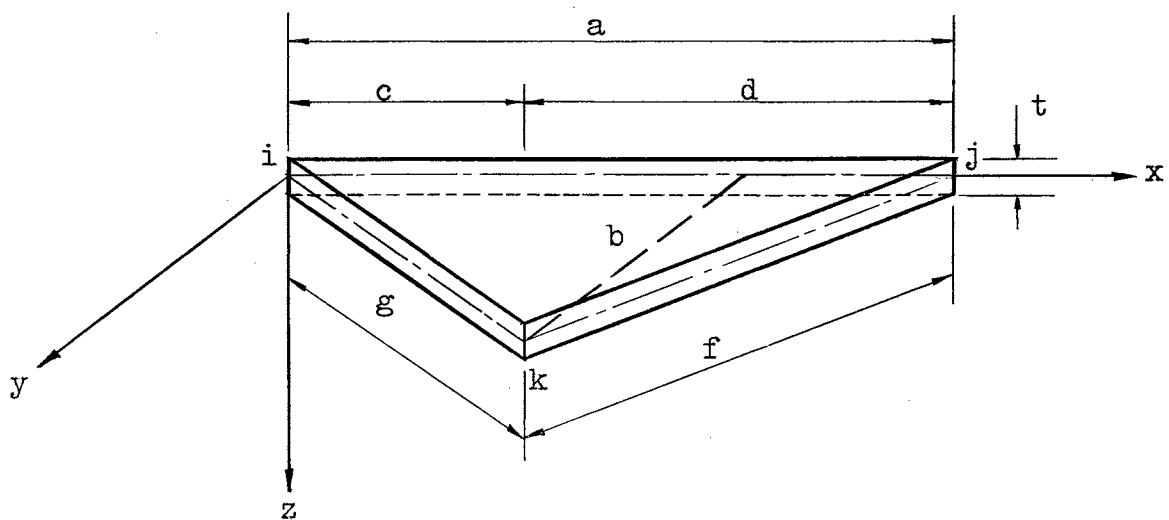


Figure 1. Element Geometry

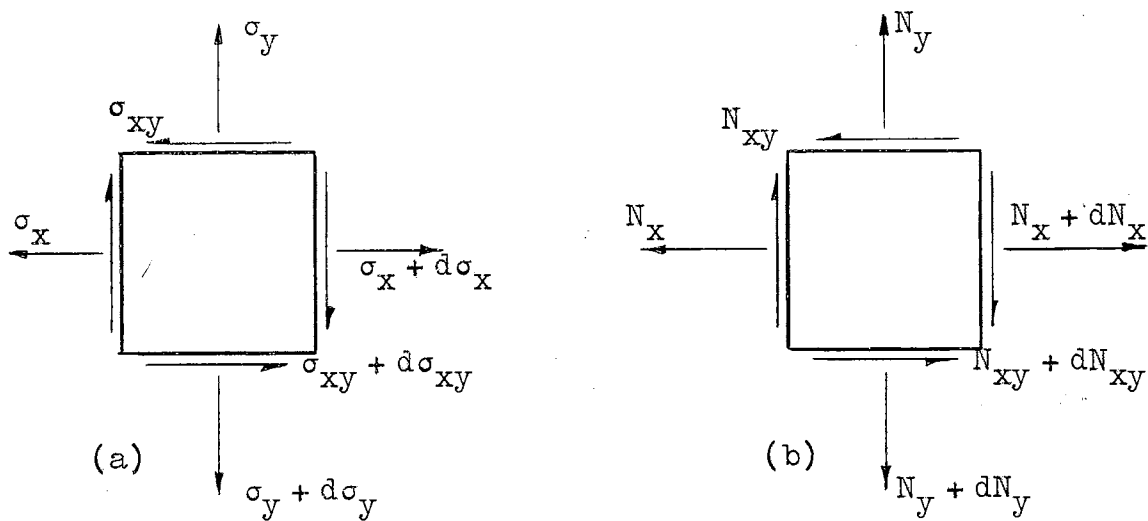


Figure 2. In-Plane Stresses and Stress Resultants

$$N_x = \int_{-t/2}^{t/2} \sigma_x dz = t(\sigma_x) \quad (2a)$$

$$N_y = \int_{-t/2}^{t/2} \sigma_y dz = t(\sigma_y) \quad (2b)$$

$$N_{xy} = \int_{-t/2}^{t/2} \sigma_{xy} dz = t(\sigma_{xy}) . \quad (2c)$$

c) Equilibrium—The assumed stress variation must satisfy the conditions of internal equilibrium:

$$\frac{\partial N_x}{\partial x} + \frac{\partial N_{xy}}{\partial y} = 0 \quad (3a)$$

$$\frac{\partial N_y}{\partial y} + \frac{\partial N_{xy}}{\partial x} = 0 . \quad (3b)$$

Performing the operations indicated in equations (3) relates six of the α 's in terms of the remaining twelve and leads to the following stress equation.

$$\{\sigma_p\} = [P_p] \{\alpha\} \quad (4)$$

The matrices of equation (4) are given in Table I.

d) Stress-strain relationship—The relationship between stresses and strains for an elastic, isotropic and homogeneous material obeying Hooke's Law may be expressed:

$$\begin{bmatrix} \epsilon_x \\ \epsilon_y \\ \gamma_{xy} \end{bmatrix} = \frac{1}{E} \begin{bmatrix} 1 & -\nu & 0 \\ -\nu & 1 & 0 \\ 0 & 0 & \frac{1}{2} \end{bmatrix} \begin{bmatrix} \sigma_x \\ \sigma_y \\ \sigma_{xy} \end{bmatrix} . \quad (5a)$$

TABLE I
STRESS FUNCTION FOR PLANE STRESS

$$\begin{bmatrix} \sigma_x \\ \sigma_y \\ \sigma_{xy} \end{bmatrix} = \begin{bmatrix} 1 & \bar{x} & \bar{y} & \bar{x}^2 & \bar{x}\bar{y} & \bar{y}^2 & 0 & 0 & 0 & 0 & 0 & 0 \\ 0 & 0 & 0 & \frac{b^2}{a^2} \bar{y}^2 & 0 & 0 & 1 & \bar{x} & \bar{y} & \bar{x}^2 & \bar{x}\bar{y} & 0 \\ 0 & -\frac{b}{a} \bar{y} & 0 & -\frac{2b}{a} \bar{x}\bar{y} & -\frac{b}{2a} \bar{y} & 0 & 0 & 0 & \frac{a}{b} \bar{x} & 0 & -\frac{a}{2b} \bar{x}^2 & 1 \end{bmatrix} \begin{bmatrix} \alpha_1 \\ \alpha_2 \\ \alpha_3 \\ \alpha_4 \\ \alpha_5 \\ \alpha_6 \\ \alpha_7 \\ \alpha_8 \\ \alpha_9 \\ \alpha_{10} \\ \alpha_{11} \\ \alpha_{13} \end{bmatrix}$$

Where: $\bar{x} = \frac{x}{a}$ $\bar{y} = \frac{y}{b}$

Where ν is the Poisson's Ratio of the material and $\bar{\nu} = 2(1 + \nu)$. Equation (5a) may simply be written as

$$\{\epsilon_p\} = [N_p] \{\sigma_p\} . \quad (5b)$$

e) Strain energy—The internal strain energy of the element may be expressed in matrix form in terms of stresses and strains.

$$\bar{U}_p = \frac{1}{2} \int_V [\sigma_p] \{\epsilon_p\} dv \quad (6a)$$

Where, as indicated, the integration is performed over the volume of the element. Using equations (4) and (5) the strain energy becomes

$$\bar{U}_p = \frac{1}{2} \int_V [\alpha] [P_p]^T [N_p] [P_p] \{\alpha\} dv . \quad (6b)$$

Since the α -vector is independent of the integration, equation (6b) may be written as

$$\bar{U}_p = \frac{1}{2} [\alpha] [H_p] \{\alpha\} \quad (6c)$$

where

$$[H_p] = \int_V [P_p]^T [N_p] [P_p] dv . \quad (7)$$

Matrices $[P_p]$ and $[N_p]$ are determined from equations (4) and (5), thus, $[H_p]$ may be evaluated. The triple matrix multiplication is performed and the elements of the resulting matrix are integrated over the volume of the triangular element. Matrix $[H_p]$ is shown in Table II and

TABLE II

MATRIX $[H_p]$

A_1	A_2	A_3	$A_4 - \frac{b^2 \bar{\nu}}{a^2} A_6$	A_5	A_6	$-\nu A_1$	$-\nu A_2$	$-\nu A_3$	$-\nu A_4$	$-\nu A_5$	0
	cc_1	A_5	$A_7 - \frac{b^2}{a^2} (2\bar{\nu} - \nu) A_8$	$A_{10} + \frac{b^2 \bar{\nu}}{2a^2} A_9$	A_8	$-\nu A_2$	$-\nu A_4$	$A_5(\bar{\nu} - \nu)$	$-\nu A_7$	$A_{10}(\frac{\bar{\nu}}{2} - \nu)$	$-\frac{b\bar{\nu}}{a} A_3$
		A_6	$A_{10} - \frac{b^2 \nu}{a^2} A_9$	A_8	A_9	$-\nu A_3$	$-\nu A_5$	$-\nu A_6$	$-\nu A_{10}$	$-\nu A_8$	0
		cc_2		$A_{13} + \frac{b^2}{a^2} (\bar{\nu} - \nu) A_{14}$	cc_3	cc_4	cc_5	cc_6	cc_7	$\frac{b^2}{a^2} A_{14} + A_{13}(\bar{\nu} - \nu)$	$-\frac{2b\bar{\nu}}{a} A_5$
				$A_{15} + \frac{b^2 \bar{\nu}}{4a^2} A_{12}$	A_{14}	$-\nu A_5$	$-\nu A_{10}$	$A_8(\frac{\bar{\nu}}{2} - \nu)$	$-\nu A_{13}$	$A_{15}(\frac{\bar{\nu}}{4} - \nu)$	$-\frac{b\bar{\nu}}{2a} A_6$
					A_{12}	$-\nu A_6$	$-\nu A_8$	$-\nu A_9$	$-\nu A_{15}$	$-\nu A_{14}$	0
					A_1	A_2	A_3	A_4	A_5		0
						A_4	A_5	A_7	A_{10}		0
							$A_6 + \frac{a^2 \bar{\nu}}{b^2} A_4$	A_{10}	$A_8 + \frac{a^2 \bar{\nu}}{2b^2} A_7$		$-\frac{a\bar{\nu}}{b} A_2$
								A_{11}	A_{13}		0
									$A_{15} + \frac{a^2 \bar{\nu}}{4b^2} A_{11}$		$-\frac{a\bar{\nu}}{2b} A_4$
											$\bar{\nu} A_1$

$$cc_1 = A_4 + \frac{b^2 \bar{\nu}}{a^2} A_6$$

$$cc_2 = A_{11} + \frac{b^4}{a^4} A_{12} + \frac{2b^2}{a^2} (2\bar{\nu} - \nu) A_{15}$$

$$cc_3 = A_{15} - \frac{b^2 \nu}{a^2} A_{12}$$

$$cc_4 = -\nu A_4 + \frac{b^2}{a^2} A_6$$

$$cc_5 = -\nu A_7 + \frac{b^2}{a^2} A_8$$

$$cc_6 = \frac{b^2}{a^2} A_9 + A_{10} (2\bar{\nu} - \nu)$$

$$cc_7 = -\nu A_{11} + \frac{b^2}{a^2} A_{15}$$

TABLE III
COEFFICIENTS FOR MATRIX $[H_p]$

$$\{A\} = \frac{bt}{120E}$$

$$\begin{bmatrix} 60a \\ 20(2c + d) \\ 20a \\ \frac{10}{a^2} (3c^3 + d^3 + 6c^2d + 4cd^2) \\ 5(3c + d) \\ 10a \\ \frac{6}{a^2} (4c^3 + 6c^2d + 4cd^2 + d^3) \\ 2(4c + d) \\ 6a \\ \frac{2}{a} (6c^2 + 4cd + d^2) \\ \frac{4}{a^2} (5c^4 + 10c^3d + 10c^2d^2 + 5cd^3 + d^4) \\ 4a \\ \frac{1}{a^2} (10c^3 + 10c^2d + 5cd^2 + d^3) \\ 5c + d \\ \frac{2}{3a} (10c^2 + 5cd + d^2) \end{bmatrix}$$

Table III.

f) Boundary displacements—The in-plane boundary displacements are assumed to vary linearly along each edge of the triangular element. They are expressed as a function of coordinate position and generalized nodal displacements. Figure 3 shows the generalized nodal displacements, U in the x -direction and V parallel to the y -axis. Edge displacements u and v for each element boundary are shown in Figure 4. They are expressed in matrix form as

$$\{u_p\} = [L_p] \{q_p\} \quad (8)$$

Where $\{u_p\}$ is the vector of in-plane edge displacements, $[L_p]$ is a coefficient matrix and $\{q_p\}$ is the vector of generalized in-plane nodal displacements. Equation (8) is recorded in Table IV.

g) Edge forces—Equivalent edge forces acting along the boundaries of the finite element are shown in Figure 5. Using stress equations (4) the edge forces are calculated in terms of the α -parameters. Letting the six edge forces shown in Figure 5 be represented by the matrix $\{S_p\}$, they can be expressed as

$$\{S_p\} = [R_p] \{\alpha\} \quad (9)$$

where

$$\{S_p\} = [N_x \ N_y \ N_\eta \ N_\xi \ N_\lambda \ N_\psi] \cdot$$

The transpose of matrix $[R_p]$ is shown in Table V.

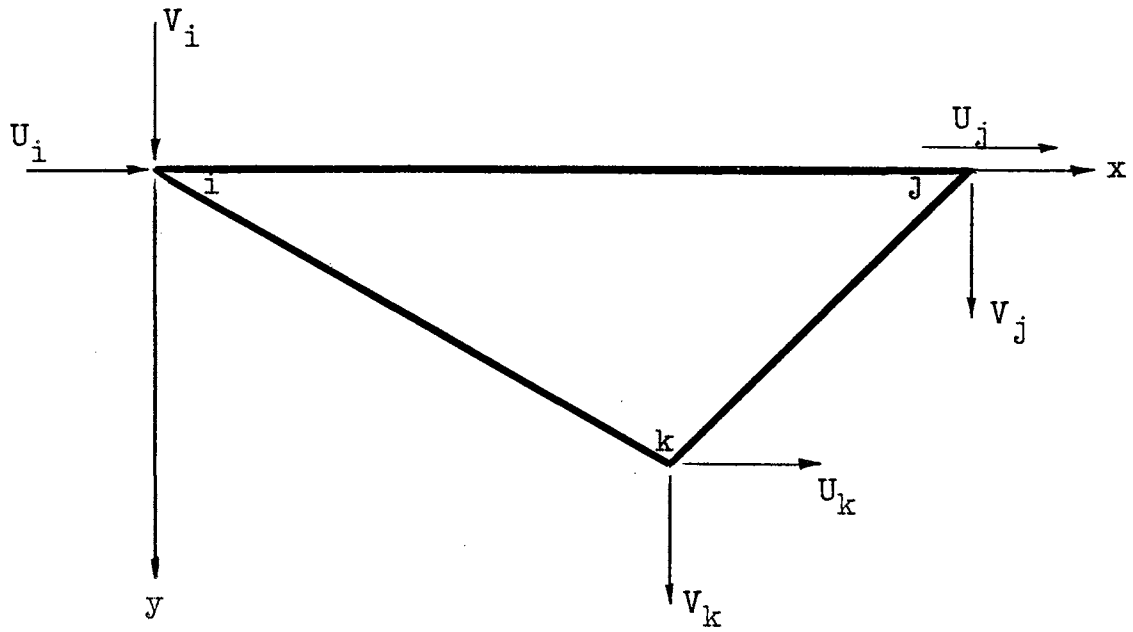


Figure 3. Generalized Nodal Displacements for Plane Stress

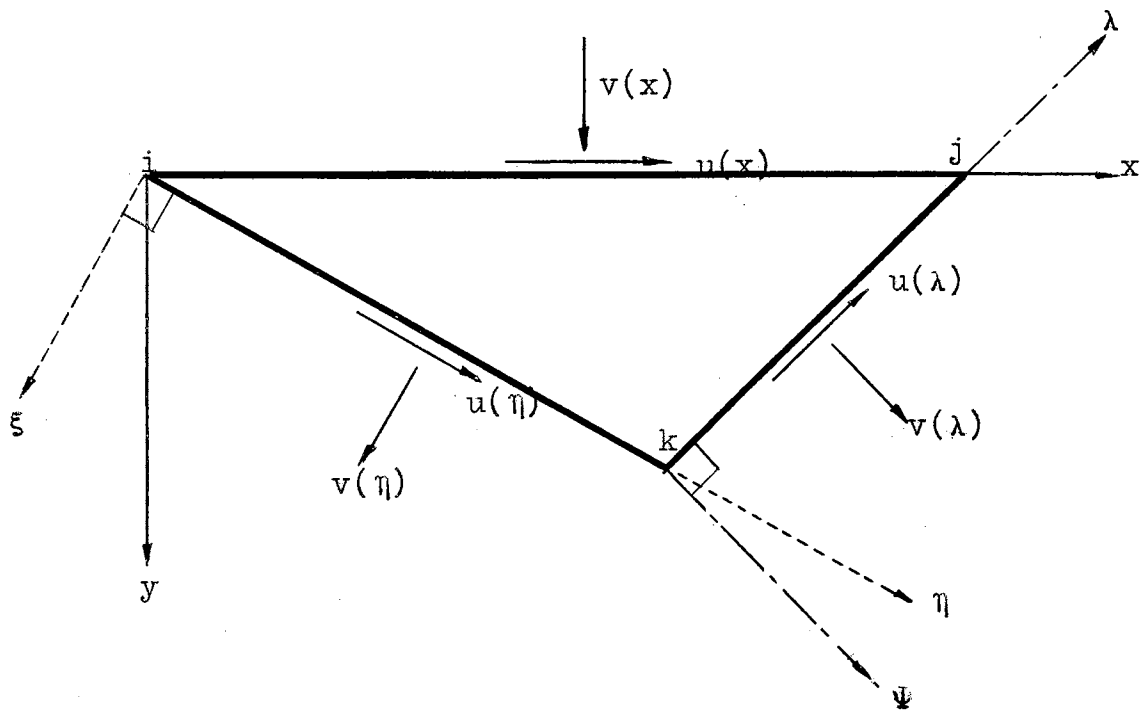


Figure 4. Edge Displacements for Plane Stress

TABLE IV
EDGE DISPLACEMENT MATRIX FOR PLANE STRESS

$$\begin{bmatrix} u(x) \\ v(x) \\ u(\eta) \\ v(\eta) \\ u(\lambda) \\ v(\lambda) \end{bmatrix} = \begin{bmatrix} 1 - \bar{x} & 0 & \bar{x} & 0 & 0 & 0 \\ 0 & 1 - \bar{x} & 0 & \bar{x} & 0 & 0 \\ \frac{c}{a} (1 - \bar{\eta}) & \frac{b}{a} (1 - \bar{\eta}) & 0 & 0 & \frac{c}{a} \bar{\eta} & \frac{b}{a} \bar{\eta} \\ \frac{b}{a} (\bar{\eta} - 1) & \frac{c}{a} (1 - \bar{\eta}) & 0 & 0 & -\frac{b}{a} \bar{\eta} & \frac{c}{a} \bar{\eta} \\ 0 & 0 & \frac{d}{c} \bar{\lambda} & -\frac{b}{c} \bar{\lambda} & \frac{d}{c} (1 - \bar{\lambda}) & \frac{b}{c} (\bar{\lambda} - 1) \\ 0 & 0 & \frac{b}{c} \bar{\lambda} & \frac{d}{c} \bar{\lambda} & -\frac{b}{c} (\bar{\lambda} - 1) & \frac{d}{c} (1 - \bar{\lambda}) \end{bmatrix} \begin{bmatrix} U_i \\ V_i \\ U_j \\ V_j \\ U_k \\ V_k \end{bmatrix}$$

Where:

$$\bar{x} = \frac{x}{a}$$

$$\bar{\eta} = \frac{a\bar{x}}{c}$$

$$\bar{\lambda} = \frac{a\bar{x} - c}{d}$$

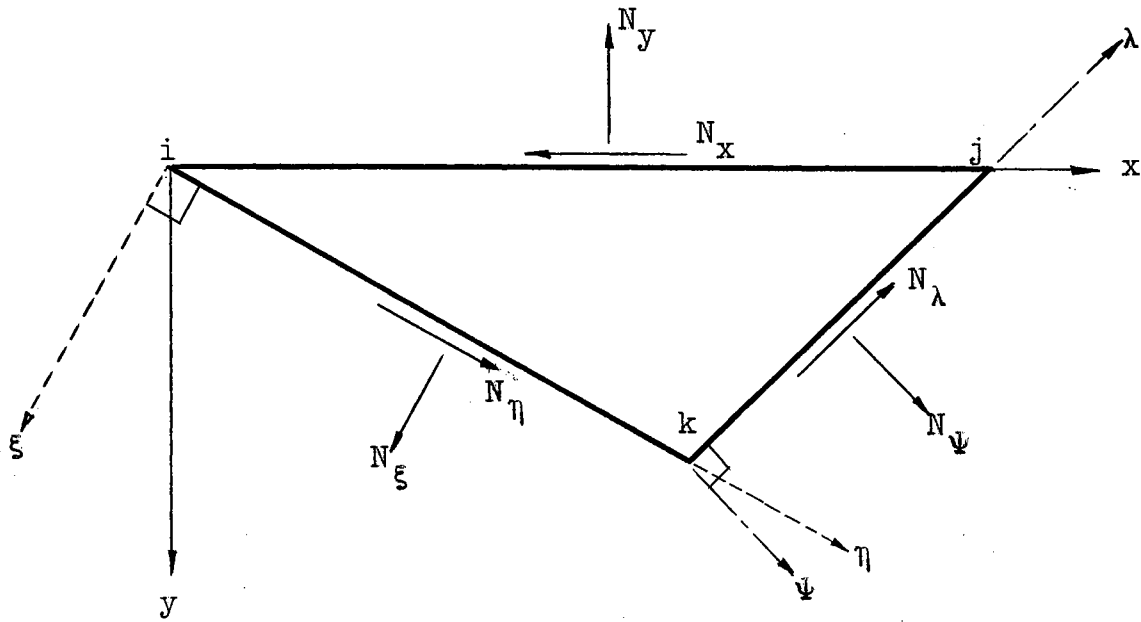


Figure 5. Edge Forces for Plane Stress

h) Work of edge forces—The boundary displacements of section (f) and edge forces of section (g) may now be employed to evaluate the work done by the edge forces. The work is conveniently expressed in matrix notation as

$$\bar{W}_p = \oint [S_p] \{u_p\} ds \quad (10)$$

where the integration is performed around the boundary of the element. Substitution of equations (8) and (9) into equation (10) yields

$$\bar{W} = \oint [\alpha] [R_p]^T [L_p] \{q_p\} ds$$

or

$$\bar{W} = [\alpha] [T_p] \{q_p\} \quad (11)$$

TABLE V

MATRIX $[R_p]^T$

t	0	$-\frac{bc}{g^2}$	$\frac{b^2}{g^2}$	$\frac{bd}{f^2}$	$\frac{b^2}{f^2}$
0	0	$\frac{b^3\bar{y}}{ag^2} - \frac{bc^2\bar{y}}{ag^2} - \frac{bc\bar{x}}{g^2}$	$\frac{b^2\bar{x}}{g^2} + \frac{2b^2c\bar{y}}{ag^2}$	$\frac{b^3\bar{y}}{af^2} - \frac{bd^2\bar{y}}{af^2} + \frac{bd\bar{x}}{f^2}$	$\frac{b^2\bar{x}}{f^2} - \frac{2b^2d\bar{y}}{af^2}$
0	0	$-\frac{b\bar{y}c}{ag^2}$	$\frac{b^2\bar{y}}{g^2}$	$\frac{bd\bar{y}}{f^2}$	$\frac{b^2\bar{y}}{f^2}$
0	0	$\frac{2b^3\bar{x}\bar{y}}{ag^2} - \frac{2bc^2\bar{x}\bar{y}}{ag^2} + \frac{b^3\bar{c}\bar{y}^2}{a^2g^2} - \frac{bc\bar{x}^2}{g^2}$	$\frac{b^2\bar{x}^2}{g^2} + \frac{b^2c\bar{y}^2}{a^2g^2} + \frac{4b^2c\bar{x}\bar{y}}{ag^2}$	$\frac{2b^3\bar{x}\bar{y}}{af^2} - \frac{2bd^2\bar{x}\bar{y}}{af^2} + \frac{bd\bar{x}^2}{f^2} - \frac{b^3d\bar{y}^2}{a^2f^2}$	$\frac{b^2\bar{x}^2}{f^2} + \frac{b^2d\bar{y}^2}{a^2f^2} - \frac{4b^2d\bar{x}\bar{y}}{af^2}$
0	0	$\frac{b^3\bar{y}^2}{2ag^2} - \frac{bc^2\bar{y}^2}{2ag^2} - \frac{bc\bar{x}\bar{y}}{g^2}$	$\frac{b^2\bar{x}\bar{y}}{g^2} + \frac{b^2c\bar{y}^2}{ag^2}$	$\frac{b^3\bar{y}^2}{2af^2} - \frac{bd^2\bar{y}^2}{2af^2} + \frac{bd\bar{x}\bar{y}}{f^2}$	$\frac{b^2\bar{x}\bar{y}}{f^2} - \frac{b^2d\bar{y}^2}{af^2}$
0	0	$-\frac{bc\bar{y}^2}{g^2}$	$\frac{b^2\bar{y}^2}{g^2}$	$\frac{bd\bar{y}^2}{f^2}$	$\frac{b^2\bar{y}^2}{f^2}$
0	-1	$\frac{bc}{g^2}$	$\frac{c^2}{g^2}$	$-\frac{bd}{f^2}$	$\frac{d^2}{f^2}$
0	$-\bar{x}$	$\frac{bc\bar{x}}{g^2}$	$\frac{c^2\bar{x}}{g^2}$	$-\frac{bd\bar{x}}{f^2}$	$\frac{d^2\bar{x}}{f^2}$
$\frac{a\bar{x}}{b}$	0	$\frac{ab\bar{x}}{g^2} - \frac{ac^2\bar{x}}{bg^2} + \frac{bc\bar{y}}{g^2}$	$\frac{c^2\bar{y}}{g^2} + \frac{2ac\bar{x}}{g^2}$	$\frac{ab\bar{x}}{f^2} - \frac{ad^2\bar{x}}{bf^2} - \frac{bd\bar{y}}{f^2}$	$\frac{d^2\bar{y}}{f^2} - \frac{2ad\bar{x}}{f^2}$
0	$-\bar{x}^2$	$\frac{bc\bar{x}^2}{g^2}$	$\frac{c^2\bar{x}^2}{g^2}$	$-\frac{bd\bar{x}^2}{f^2}$	$\frac{d^2\bar{x}^2}{f^2}$
$\frac{a\bar{x}^2}{2b}$	0	$\frac{ab\bar{x}^2}{2g^2} - \frac{ac^2\bar{x}^2}{2bg^2} + \frac{bc\bar{x}\bar{y}}{g^2}$	$\frac{c^2\bar{x}\bar{y}}{g^2} + \frac{ac\bar{x}^2}{g^2}$	$\frac{ab\bar{x}^2}{2f^2} - \frac{ad^2\bar{x}^2}{2bf^2} - \frac{bd\bar{x}\bar{y}}{f^2}$	$\frac{d^2\bar{x}\bar{y}}{f^2} - \frac{ad\bar{x}^2}{f^2}$
-1	0	$\frac{c^2 - b^2}{g^2}$	$-\frac{2bc}{g^2}$	$\frac{d^2 - b^2}{f^2}$	$\frac{2bd}{f^2}$

where

$$[T_p] = \oint [R_p]^T [L_p] ds . \quad (12)$$

The matrix multiplication indicated in equation (12) is first performed and the elements of the resulting matrix are then integrated along the appropriate edge. $[T_p]$ is shown in Table VI.

i) Complementary energy—Having formulated the internal strain energy and the work of the edge forces, the complementary energy may now be formulated.

$$\pi_{cp} = \bar{U}_p - \bar{W}_p \quad (13)$$

Equations (6c) and (12) are substituted into (13) to obtain

$$\pi_{cp} = \frac{1}{2} [\alpha] [H_p] \{\alpha\} - [\alpha] [T_p] \{q_p\} . \quad (14)$$

The principle of minimum complementary energy requires

$$\frac{\partial \pi_{cp}}{\partial \alpha_m} = 0 \quad (\text{For all } \alpha_m) . \quad (15)$$

Therefore

$$[H_p] \{\alpha\} = [T_p] \{q_p\} . \quad (16)$$

j) Element stiffness matrix—Equation (16) may be solved for $\{\alpha\}$ to yield

$$\{\alpha\} = [H_p]^{-1} [T_p] \{q_p\} . \quad (17)$$

Equation (17) is substituted into equation (6c) to obtain the following expression for strain energy.

TABLE VI
MATRIX $[T_p]$

t	$-\frac{b}{2}$	0	$\frac{b}{2}$	0	0	0
	$-\frac{bc}{3a}$	$\frac{b^2}{6a}$	$\frac{b}{6a}(3c+d)$	$-\frac{b^2}{6a}$	$-\frac{b}{6}$	0
	$-\frac{b}{6}$	0	$\frac{b}{6}$	0	0	0
	$-\frac{bc^2}{4a^2}$	$\frac{b^2c}{4a^2}$	$\frac{b}{12a^2}(6c^2+d^2+4cd)$	$-\frac{b^2}{12a^2}(4c+d)$	$-\frac{b}{12a}(3c+d)$	$\frac{b^2}{12a}$
	$-\frac{bc}{8a}$	$\frac{b^2}{24a}$	$\frac{b}{24a}(4c+d)$	$-\frac{b^2}{24a}$	$-\frac{b}{24}$	0
	$-\frac{b}{12}$	0	$\frac{b}{12}$	0	0	0
	0	$-\frac{d}{2}$	0	$-\frac{c}{2}$	0	$\frac{a}{2}$
	0	$-\frac{d}{6a}(2c+d)$	0	$-\frac{c}{6a}(2c+d)$	0	$\frac{1}{6}(2c+d)$
	$\frac{d}{6b}(a+c)$	$\frac{c}{3}$	$\frac{c}{6b}(2c+d)$	$-\frac{1}{6}(3c+d)$	$-\frac{a}{6b}(2c+d)$	$\frac{a}{6}$
	0	$\frac{1}{12a^2}(c^3-a^3)$	0	$\frac{1}{12a^2}(-3a^3+6c^2d+8cd^2+3d^3)$	0	$\frac{1}{12a^2}(3c^3+6c^2d+4cd^2+d^3)$
	$\frac{1}{24ab}(a^3-c^3)$	$\frac{c^2}{8a}$	$\frac{c}{24ab}(3c^2+3cd+d^2)$	$-\frac{1}{24a}(6c^2+4cd+d^2)$	$-\frac{1}{24ab}(3c^3+6c^2d+4cd^2+d^3)$	$\frac{1}{24}(3c+d)$
	$-\frac{d}{2}$	$-\frac{b}{2}$	$-\frac{c}{2}$	$\frac{b}{2}$	$\frac{a}{2}$	0

$$\bar{U}_p = \frac{1}{2} [q_p]^T [T_p]^T [H_p]^{-1} [T_p] \{q_p\} \quad (18)$$

If $[K_p]$ represents the matrix of stiffness coefficients, strain energy may also be expressed as

$$\bar{U}_p = \frac{1}{2} [q_p]^T [K_p] \{q_p\} . \quad (19)$$

Comparison of equations (18) and (19) yields the stiffness matrix of the element in terms of $[H_p]$ and $[T_p]$:

$$[K_p] = [T_p]^T [H_p]^{-1} [T_p] . \quad (20)$$

Equation (20) represents the end product sought in this section. It is the plane stress stiffness matrix referenced with respect to the elemental system of axes.

In the following section, a similar procedure is employed to develop a bending stiffness matrix.

2.3 Bending Stiffness Matrix

a) Stress functions—For any point in the triangular element of Figure 1 it is assumed that the five stress components σ_x , σ_y , σ_{xy} , σ_{zx} , σ_{zy} may be expressed as a function of the coordinates of the point and a set of parameters, β_m . σ_x , σ_y and σ_{xy} are assumed to have a linear variation across the depth of the element and a quadratic variation in the plane of the element. σ_{zx} and σ_{zy} have a parabolic variation across the depth of the element and a linear variation in the plane of the element. Figure 6 shows

the assumed stress variation across the element thickness.

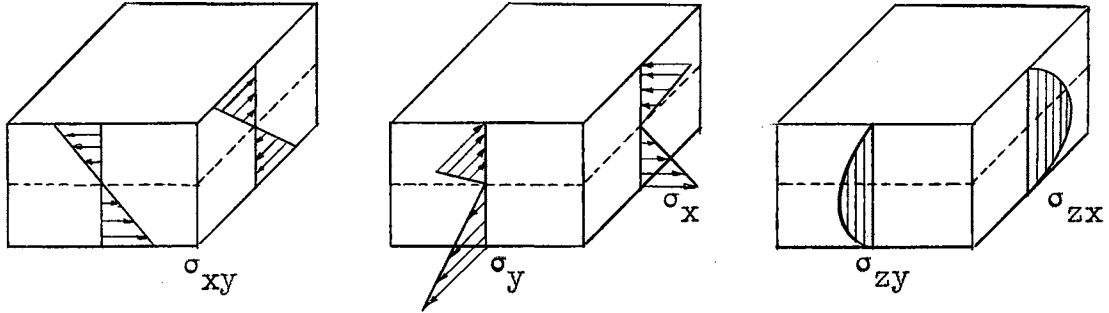


Figure 6. Bending Stress Distribution

The five stress equations are:

$$\sigma_x = \bar{Z} (\beta_1 + \beta_2 \bar{x} + \beta_3 \bar{y} + \beta_4 \bar{x}^2 + \beta_5 \bar{x}\bar{y} + \beta_6 \bar{y}^2) \quad (21a)$$

$$\sigma_y = \bar{Z} (\beta_7 + \beta_8 \bar{x} + \beta_9 \bar{y} + \beta_{10} \bar{x}^2 + \beta_{11} \bar{x}\bar{y} + \beta_{12} \bar{y}^2) \quad (21b)$$

$$\sigma_{xy} = \bar{Z} (\beta_{13} + \beta_{14} \bar{x} + \beta_{15} \bar{y} + \beta_{16} \bar{x}^2 + \beta_{17} \bar{x}\bar{y} + \beta_{18} \bar{y}^2) \quad (21c)$$

$$\sigma_{zx} = Z' (\beta_{19} + \beta_{20} \bar{x} + \beta_{21} \bar{y}) \quad (21d)$$

$$\sigma_{zy} = Z' (\beta_{22} + \beta_{23} \bar{x} + \beta_{24} \bar{y}) \quad (21e)$$

Where

$$\bar{Z} = \frac{8z}{t}$$

$$Z' = 1 - \frac{4z^2}{t^2}$$

and \bar{x} and \bar{y} are as previously defined.

Having assumed stress equations (21), the stress resultants may be determined.

b) Stress resultants—The five stress resultants are

determined by integrating equations (21) across the depth of the element.

$$M_x = \int_{-t/2}^{t/2} \sigma_x z dz = \frac{2t^2}{3} (\beta_1 + \beta_2 \bar{x} + \beta_3 \bar{y} + \beta_4 \bar{x}^2 + \beta_5 \bar{x}\bar{y} + \beta_6 \bar{y}^2) \quad (22a)$$

$$M_y = \int_{-t/2}^{t/2} \sigma_y z dz = \frac{2t^2}{3} (\beta_7 + \beta_8 \bar{x} + \beta_9 \bar{y} + \beta_{10} \bar{x}^2 + \beta_{11} \bar{x}\bar{y} + \beta_{12} \bar{y}^2) \quad (22b)$$

$$M_{xy} = \int_{-t/2}^{t/2} \sigma_{xy} z dz = \frac{2t^2}{3} (\beta_{13} + \beta_{14} \bar{x} + \beta_{15} \bar{y} + \beta_{16} \bar{x}^2 + \beta_{17} \bar{x}\bar{y} + \beta_{18} \bar{y}^2) \quad (22c)$$

$$Q_{zx} = \int_{-t/2}^{t/2} \sigma_{zx} dz = \frac{2t}{3} (\beta_{19} + \beta_{20} \bar{x} + \beta_{21} \bar{y}) \quad (22d)$$

$$Q_{zy} = \int_{-t/2}^{t/2} \sigma_{zy} dz = \frac{2t}{3} (\beta_{22} + \beta_{23} \bar{x} + \beta_{24} \bar{y}) \quad (22e)$$

c) Equilibrium—Application of the conditions of equilibrium of the element shown in Figure 7 allows for seven β -parameters to be solved for in terms of the remaining seventeen. Equations of equilibrium to be satisfied are

$$\frac{\partial Q_x}{\partial x} + \frac{\partial Q_y}{\partial y} = 0 \quad (23a)$$

$$\frac{\partial M_y}{\partial y} + \frac{\partial M_{xy}}{\partial x} - Q_{zy} = 0 \quad (23b)$$

$$\frac{\partial M_x}{\partial x} + \frac{\partial M_{xy}}{\partial y} - Q_{zx} = 0 \quad (23c)$$

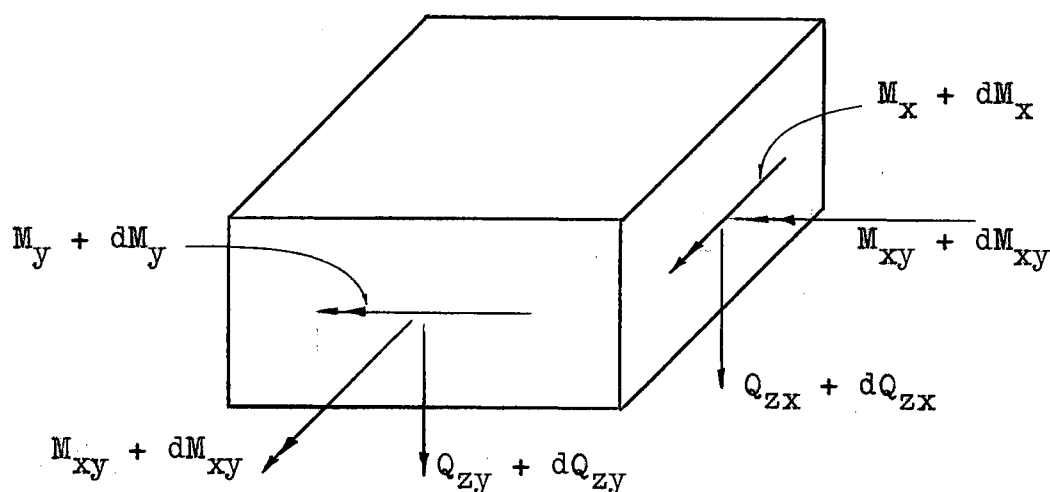


Figure 7. Bending Stress Resultants

Equations (22) are substituted into (23) to obtain the relationship between the β parameters. In terms of the reduced number of β 's, stress equations (21) may now be expressed as

$$\{\sigma_b\} = [P_b] \{\beta\} . \quad (24)$$

Where

$$\{\sigma_b\} = \{\sigma_x, \sigma_y, \sigma_{xy}, \sigma_{zx}, \sigma_{zy}\} ,$$

$$\{\beta\} = \{\beta_1, \beta_2, \beta_3, \dots, \beta_{16}, \beta_{18}\} ,$$

and matrix $[P_b]$ is as shown in Table VII.

d) Stress-strain relationship—The stress-strain relationship for an elastic, isotropic and homogeneous material obeying Hooke's Law may be expressed in the following manner:

TABLE VII
MATRIX $[P_b]$

\bar{z}	\bar{zx}	\bar{zy}	\bar{zx}^2	\bar{zxy}	\bar{zy}^2	0	0	0	0	0	0	0	0	0	0	0
0	0	0	0	0	0	\bar{z}	\bar{zx}	\bar{zy}	\bar{zx}^2	\bar{zxy}	\bar{zy}^2	0	0	0	0	0
0	0	0	$-\frac{b}{a} \bar{zxy}$	0	0	0	0	0	0	0	$-\frac{a}{b} \bar{zxy}$	\bar{z}	\bar{zx}	\bar{zy}	\bar{zx}^2	\bar{zy}^2
0	$\frac{1}{a} z'$	0	$\frac{1}{a} z' \bar{x}$	$\frac{1}{a} z' \bar{y}$	0	0	0	0	0	0	$-\frac{a}{b^2} z' \bar{x}$	0	0	$\frac{1}{b} z'$	0	$\frac{2}{b} z' \bar{y}$
0	0	0	$-\frac{b}{a^2} z' \bar{y}$	0	0	0	$\frac{1}{b} z'$	0	$\frac{1}{b} z' \bar{x}$	$\frac{1}{b} z' \bar{y}$	0	$\frac{1}{a} z'$	0	$\frac{2}{a} z' \bar{x}$	0	0

$$\begin{bmatrix} \epsilon_x \\ \epsilon_y \\ \gamma_{xy} \\ \gamma_{zx} \\ \gamma_{zy} \end{bmatrix} = \frac{1}{E} \begin{bmatrix} 1 & -\nu & 0 & 0 & 0 \\ -\nu & 1 & 0 & 0 & 0 \\ 0 & 0 & \bar{\nu} & 0 & 0 \\ 0 & 0 & 0 & \bar{\nu} & 0 \\ 0 & 0 & 0 & 0 & \bar{\nu} \end{bmatrix} \begin{bmatrix} \sigma_x \\ \sigma_y \\ \sigma_{xy} \\ \sigma_{zx} \\ \sigma_{zy} \end{bmatrix} \quad (25a)$$

or, more concisely as

$$\{\epsilon_b\} = [N_b] \{\sigma_b\}. \quad (25b)$$

e) Strain energy—Referring to equation (6) the expression for strain energy due to bending may be written:

$$\bar{U}_b = \frac{1}{2} [\beta] [H_b] \{\beta\} \quad (26)$$

where

$$[H_b] = \int_v [P_b]^T [N_b] [P_b] dv. \quad (27)$$

The matrix $[H_b]$ is evaluated in the same manner as for the plane stress condition and is presented in Table VIII and Table IX.

f) Boundary displacements—Expressions for boundary displacements are assumed such that compatibility of the three deformations along a line separating two elements is achieved. That is, compatibility of the vertical deflection and the slopes, normal and tangent to the line. Edge displacements are expressed in terms of the generalized nodal displacements at the ends of the line. Consider a general

TABLE VIII
MATRIX $[H_b]$

A_1	A_2	A_3	A_4	A_5	A_6	$-vA_1$	$-vA_2$	$-vA_3$	$-vA_4$	$-vA_5$	$-vA_6$	0	0	0	0	0
$A_4 + \frac{v}{a^2}A_{16}$	A_5	$A_7 + \frac{v}{a^2}A_{17}$	$A_{10} + \frac{v}{a^2}A_{18}$	A_8	$-vA_2$	$-vA_4$	$-vA_5$	$-vA_7$	$-vA_{10}$	$-vA_8 + \frac{v}{b^2}A_{17}$	0	0	$\frac{v}{ab}A_{16}$	0	$\frac{2v}{ab}A_{18}$	
	A_6	A_{10}	A_8	A_9	$-vA_3$	$-vA_5$	$-vA_6$	$-vA_{10}$	$-vA_8$	$-vA_9$	0	0	0	0	0	
	BB_1	$A_{13} + \frac{v}{a^2}A_{19}$	A_{15}	$-vA_4$	$-vA_7$	$-vA_{10} + \frac{v}{a^2}A_{18}$	$-vA_{11}$	$-vA_{13} + \frac{v}{a^2}A_{19}$	BB_2	$-\frac{bv}{a}A_5 - \frac{bv}{a}(A_{10} + \frac{1}{a^2}A_{18})$	$\frac{v}{a}(-bA_8 + \frac{1}{b^2}A_{17})$	$-\frac{bv}{a}(A_{13} + \frac{2}{a^2}A_{19})$	$-\frac{v}{a}(bA_{14} + \frac{2}{b^2}A_{19})$			
		$A_{15} + \frac{v}{a^2}A_{21}$	A_{14}	$-vA_5$	$-vA_{10}$	$-vA_8$	$-vA_{13}$	$-vA_{15}$	$-vA_{14} + \frac{v}{b^2}A_{19}$	0	0	$\frac{v}{ab}A_{18}$	0	$\frac{2v}{ab}A_{21}$		
			A_{12}	$-vA_6$	$-vA_8$	$-vA_9$	$-vA_{15}$	$-vA_{14}$	$-vA_{12}$	0	0	0	0	0		
$BB_1 = A_{11} + \frac{v}{a^2}(b^2A_{15} + \frac{1}{a^2}A_{21})$			A_1	A_2	A_3	A_4	A_5	A_6	0	0	0	0	0	0		
$BB_2 = A_{15}(\bar{v} - v) - \frac{v}{b^2}A_{20} + \frac{v}{a^2}A_{21}$			A_4	A_5	A_7	A_{10}	A_8	0	0	0	0	0	0	0		
$BB_3 = A_{12} + \frac{v}{b^2}(a^2A_{15} + \frac{b^2}{a^2}A_{20} + A_{21})$			$A_6 + \frac{v}{b^2}A_{16}$	A_{10}	$A_8 + \frac{v}{b^2}A_{17}$	$A_9 + \frac{v}{b^2}A_{18}$	0	$\frac{v}{ab}A_{16}$	0	$\frac{2v}{ab}A_{17}$	0	$\frac{2v}{ab}A_{18}$	0			
				A_{11}	A_{13}	A_{15}	0	0	0	0	0	0	0			
					$A_6 + \frac{v}{b^2}A_{20}$	$A_{14} + \frac{v}{b^2}A_{19}$	0	$\frac{v}{ab}A_{17}$	0	$\frac{2v}{ab}A_{20}$	0					
						BB_3	$-\frac{bv}{b}A_5$	$\frac{v}{b}(-bA_{10} + \frac{1}{a^2}A_{18})$	$-\frac{bv}{b}(A_8 + \frac{1}{b^2}A_{17})$	$\frac{v}{b}(-bA_8 + \frac{2}{a^2}A_{19})$	$-\frac{bv}{b}(A_{14} + \frac{2}{b^2}A_{19})$					
							$\bar{v}A_1$	$\bar{v}A_2$	$\bar{v}A_3$	$\bar{v}A_4$	$\bar{v}A_6$					
								$\bar{v}A_4 + \frac{v}{a^2}A_{16}$	$\bar{v}A_5$	$\bar{v}A_7 + \frac{2v}{a^2}A_{17}$	$\bar{v}A_8$					
									$\bar{v}A_8 + \frac{v}{b^2}A_{16}$	$\bar{v}A_{10}$	$\bar{v}A_9 + \frac{2v}{b^2}A_{18}$					
										$\bar{v}A_{11} + \frac{4v}{a^2}A_{20}$	$\bar{v}A_{15}$					
											$\bar{v}A_{12} + \frac{4v}{b^2}A_{21}$					

(SYMMETRICAL)

TABLE IX
COEFFICIENTS FOR MATRIX $[H_b]$

$$\{A\} = \frac{8abt}{3E}$$

$$\left[\begin{array}{l} 1 \\ \frac{a+c}{3a} \\ \frac{1}{3} \\ \frac{3c^2 + 3cd + d^2}{6a^2} \\ \frac{3c+d}{12a} \\ \frac{1}{6} \\ \frac{4c^3 + d^3 + 6c^2d + 4cd^2}{10a^3} \\ \frac{4c+d}{30a} \\ \frac{1}{10} \\ \frac{6c^2 + 4cd + d^2}{30a^2} \\ \frac{5c^4 + 10c^3d + 10c^2d^2 + 5cd^3 + d^4}{15a^4} \\ \frac{1}{15} \\ \frac{10c^3 + 10c^2d + 5cd^2 + d^3}{60a^3} \\ \frac{5c+d}{60a} \\ \frac{10c^2 + 5cd + d^2}{90a^2} \\ \frac{t^2}{10} \\ \frac{t^2(a+c)}{30a} \\ \frac{t^2}{30} \\ \frac{t^2(3c+d)}{120a} \\ \frac{t^2(3c^2 + 3cd + d^2)}{60a^2} \\ \frac{t^2}{60} \end{array} \right]$$

edge st shown in Figure 8. The orthogonal axes system has a general orientation.

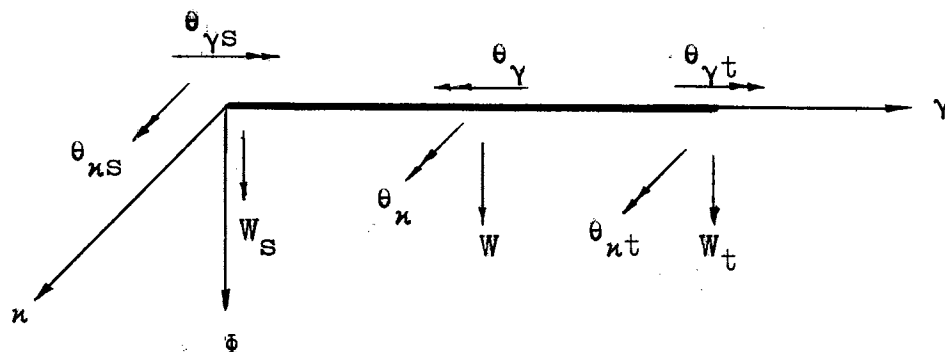


Figure 8. General Displacements

Vertical deflection along st is represented by a third degree polynomial in γ .

$$W(\gamma) = A_0 + A_1\gamma + A_2\gamma^2 + A_3\gamma^3 \quad (28a)$$

This polynomial involves four constants which may be evaluated in terms of the four nodal displacements W_s , θ_{ns} , W_t and θ_{nt} . The torsional rotation θ_γ is assumed to vary linearly along st and is expressed in terms of $\theta_{\gamma s}$ and $\theta_{\gamma t}$ as

$$\theta_\gamma = \theta_{\gamma i} (\gamma - 1) - \theta_{\gamma j} \bar{\gamma} \quad (28b)$$

where

$$\bar{\gamma} = \frac{\gamma}{st}.$$

Equations (28) are applied to each of the three edges of

the triangular element shown in Figure 9. This yields a set of nine equations which are most conveniently expressed in matrix form

$$\{u_b\} = [L_b] \{q_b\} . \quad (29)$$

Where $\{u_b\}$ is the vector of edge displacements, $[L_b]$ is a coefficient matrix and $\{q_b\}$ is the vector of generalized nodal displacements. The generalized nodal displacements are shown in Figure 10. Equation (29) is recorded in Table X.

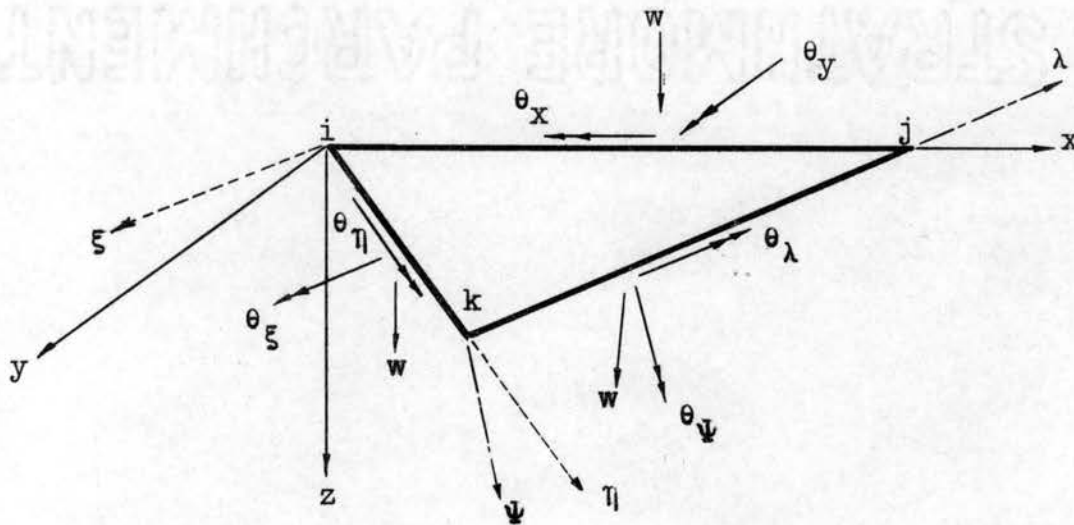


Figure 9. Boundary Displacements Due to Bending

g) Edge actions—Equivalent edge actions are shown in Figure 11. They are evaluated from the stress equations (24)

TABLE X

EDGE DISPLACEMENT MATRIX FOR BENDING

θ_{xij}	$(\bar{x}-1)$	0	0	$-\bar{x}$	0	0	0	0	0	θ_{xi}
θ_{yij}	0	$(1-4\bar{x}+3\bar{x}^2)$	$\frac{6}{a}(\bar{x}-\bar{x}^2)$	0	$(-2\bar{x}+3\bar{x}^2)$	$\frac{6}{2}(-\bar{x}+\bar{x}^2)$	0	0	0	θ_{yi}
w_{ij}	0	$a(-\bar{x}+2\bar{x}^2-\bar{x}^3)$	$(1-3\bar{x}^2+2\bar{x}^3)$	0	$a(\bar{x}^2-\bar{x}^3)$	$(3\bar{x}^2-2\bar{x}^3)$	0	0	0	w_i
$\theta_{\eta ik}$	$\frac{c}{a}(1-\bar{\eta})$	$\frac{b}{a}(1-\bar{\eta})$	0	0	0	0	$\frac{c}{a}\bar{\eta}$	$\frac{b}{a}\bar{\eta}$	0	θ_{xj}
$\theta_{\xi ik}$	$\frac{b}{a}(-1+4\bar{\eta}-3\bar{\eta}^2)$	$\frac{c}{a}(1-4\bar{\eta}+3\bar{\eta}^2)$	$\frac{6}{a}(\bar{\eta}-\bar{\eta}^2)$	0	0	0	$\frac{b}{a}(+2\bar{\eta}-3\bar{\eta}^2)$	$\frac{c}{a}(-2\bar{\eta}+3\bar{\eta}^2)$	$\frac{6}{a}(-\bar{\eta}+\bar{\eta}^2)$	θ_{yj}
w_{ik}	$b(\bar{\eta}-2\bar{\eta}^2+\bar{\eta}^3)$	$c(-\bar{\eta}+2\bar{\eta}^2-\bar{\eta}^3)$	$(1-3\bar{\eta}^2+2\bar{\eta}^3)$	0	0	0	$b(-\bar{\eta}^2+\bar{\eta}^3)$	$c(\bar{\eta}^2-\bar{\eta}^3)$	$(3\bar{\eta}^2-2\bar{\eta}^3)$	w_j
$\theta_{\lambda jk}$	0	0	0	$-\frac{d}{f}\bar{\lambda}$	$\frac{b}{f}\bar{\lambda}$	0	$\frac{d}{f}(\bar{\lambda}-1)$	$\frac{b}{f}(1-\bar{\lambda})$	0	θ_{xk}
$\theta_{\psi jk}$	0	0	0	$\frac{b}{f}(-2\bar{\lambda}+3\bar{\lambda}^2)$	$\frac{d}{f}(-2\bar{\lambda}+3\bar{\lambda}^2)$	$\frac{6}{f}(-\bar{\lambda}+\bar{\lambda}^2)$	$\frac{b}{f}(1-4\bar{\lambda}+3\bar{\lambda}^2)$	$\frac{d}{f}(1-4\bar{\lambda}+3\bar{\lambda}^2)$	$\frac{6}{f}(\bar{\lambda}-\bar{\lambda}^2)$	θ_{yk}
w_{jk}	0	0	0	$b(\bar{\lambda}^2-\bar{\lambda}^3)$	$d(\bar{\lambda}^2-\bar{\lambda}^3)$	$(3\bar{\lambda}^2-2\bar{\lambda}^3)$	$b(-\bar{\lambda}+2\bar{\lambda}^2-\bar{\lambda}^3)$	$d(-\bar{\lambda}+2\bar{\lambda}^2-\bar{\lambda}^3)$	$(1-3\bar{\lambda}^2+2\bar{\lambda}^3)$	w_k

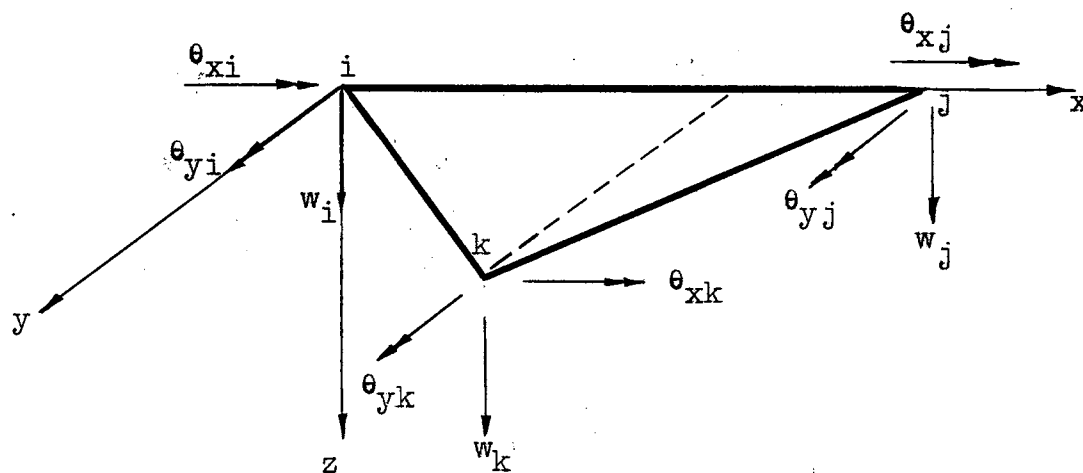


Figure 10. Generalized Nodal Displacements Due to Bending

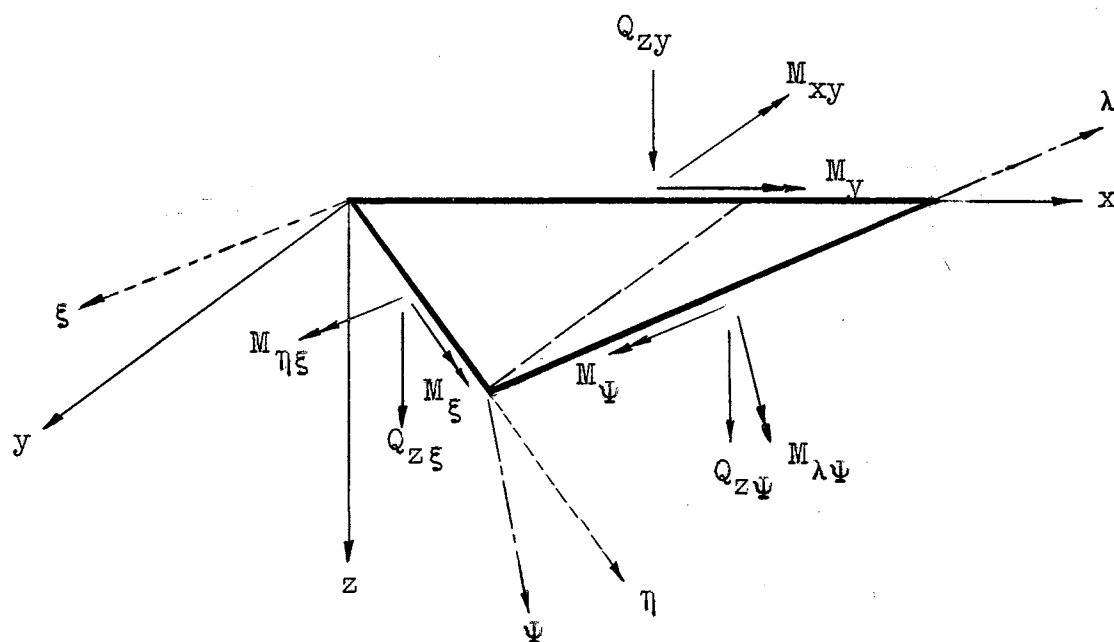


Figure 11. Edge Actions Due to Bending

and expressed in matrix notation as

$$\{S_b\} = [R_b] \{\beta\} \quad (30)$$

where $\{S_b\}$ is the vector of edge actions due to bending and $[R_b]$ is a coefficient matrix. The transpose of $[R_b]$ is presented in Table XI.

h) Work of edge actions—As previously discussed in connection with equation (10) the work of the bending edge actions acting through their respective displacements may be expressed as

$$\bar{W}_b = [\beta] [T_b] \{q_b\} \quad (31)$$

where

$$[T_b] = \oint [R_b]^T [L_b] ds. \quad (32)$$

The elements of matrix $[T_b]$ are listed in Appendix A.

i) Complementary energy—Applying the principle of minimum complementary energy leads to results similar to equation (16). The following expression is obtained:

$$[H_b] \{\beta\} = [T_b] \{q_b\}. \quad (33)$$

j) Element stiffness matrix in bending—The matrix algebra involved here is the same as in paragraph (j) of section 2.2 and results in the following equation:

$$[K_b] = [T_b]^T [H_b]^{-1} [T_b]. \quad (34)$$

Equation (34) represents the bending stiffness matrix referenced with respect to the elemental system of axes,

TABLE XI
MATRIX $[R_b]^T$

0	0	0	$-\frac{b^2}{g^2}$	$-\frac{bc}{g^2}$	0	$\frac{b^2}{f^2}$	$\frac{bd}{f^2}$	0	$\frac{2t^2}{3}$
0	0	0	$-\frac{b^2\bar{x}}{g^2}$	$-\frac{bc\bar{x}}{g^2}$	$-\frac{b}{ag}$	$\frac{b^2\bar{x}}{f^2}$	$\frac{bd\bar{x}}{f^2}$	$\frac{b}{af}$	
0	0	0	$-\frac{ab^2\bar{x}}{cg^2}$	$-\frac{ab\bar{x}}{g^2}$	0	$\frac{ab^2}{df^2}M_1$	$\frac{ab}{f^2}M_1$	0	
0	0	0	$-\frac{3b^2\bar{x}^2}{g^2}$	$\frac{b\bar{x}^2}{cg^2}(b^2 - 2c^2)$	$-\frac{2b\bar{x}}{ag}$	$\frac{b^2}{f^2}M_2$	$\frac{b}{f^2}(\frac{b^2}{d}M_4 - dM_3)$	$\frac{b}{af}M_5$	
0	0	0	$-\frac{ab^2\bar{x}^2}{cg^2}$	$-\frac{ab\bar{x}^2}{g^2}$	$-\frac{b\bar{x}}{cg}$	$\frac{ab^2}{df^2}M_4$	$\frac{ab}{f^2}M_4$	$\frac{b}{df}M_1$	
0	0	0	$-\frac{a^2b^2\bar{x}^2}{c^2g^2}$	$-\frac{a^2b\bar{x}^2}{cg^2}$	0	$\frac{a^2b^2}{d^2f^2}M_6$	$\frac{a^2b}{df^2}M_6$	0	
-1	0	0	$-\frac{c^2}{g^2}$	$\frac{bc}{g^2}$	0	$\frac{d^2}{f^2}$	$-\frac{bd}{f^2}$	0	
$-\bar{x}$	0	0	$-\frac{c^2\bar{x}}{g^2}$	$\frac{bc\bar{x}}{g^2}$	0	$\frac{d^2\bar{x}}{f^2}$	$-\frac{bd\bar{x}}{f^2}$	0	
0	0	$-\frac{1}{b}$	$-\frac{ac\bar{x}}{g^2}$	$\frac{ab\bar{x}}{g^2}$	$\frac{c}{bg}$	$\frac{ad}{f^2}M_1$	$-\frac{ab}{f^2}M_1$	$\frac{d}{bf}$	
$-\bar{x}^2$	0	0	$-\frac{c^2\bar{x}^2}{g^2}$	$\frac{bc\bar{x}^2}{g^2}$	0	$\frac{d^2\bar{x}^2}{f^2}$	$-\frac{bd\bar{x}^2}{f^2}$	0	
0	0	$-\frac{\bar{x}}{b}$	$-\frac{ac\bar{x}^2}{g^2}$	$\frac{ab\bar{x}^2}{g^2}$	$\frac{c\bar{x}}{bg}$	$\frac{ad}{f^2}M_4$	$-\frac{ab}{f^2}M_4$	$\frac{d\bar{x}}{bf}$	
0	0	0	$-\frac{3a^2\bar{x}^2}{g^2}$	$\frac{a^2\bar{x}^2}{bcg^2}(2b^2 - c^2)$	$\frac{2a\bar{x}}{bg}$	$\frac{a^2}{f^2}M_7$	$-\frac{a^2}{f^2}(\frac{b}{d}M_8 + dM_4)$	$\frac{a}{bf}M_5$	
0	-1	0	$\frac{2bc}{g^2}$	$\frac{c^2 - b^2}{g^2}$	0	$\frac{2bd}{f^2}$	$\frac{d^2 - b^2}{f^2}$	0	
0	$-\bar{x}$	$-\frac{1}{a}$	$\frac{2bc\bar{x}}{g^2}$	$\frac{c^2 - b^2}{g^2}\bar{x}$	$\frac{c}{ag}$	$\frac{2bd\bar{x}}{f^2}$	$\frac{d^2 - b^2}{f^2}\bar{x}$	$\frac{d}{af}$	
0	0	0	$\frac{2ab\bar{x}}{g^2}$	$\frac{ac^2 - ab^2}{cg^2}\bar{x}$	$-\frac{1}{g}$	$\frac{2ab}{f^2}M_1$	$\frac{a(d^2 - b^2)}{df^2}M_1$	$\frac{1}{f}$	
0	$-\bar{x}^2$	$-\frac{2\bar{x}}{a}$	$\frac{2bc\bar{x}^2}{g^2}$	$\frac{c^2 - b^2}{g^2}\bar{x}^2$	$\frac{2c\bar{x}}{ag}$	$\frac{2bd\bar{x}^2}{f^2}$	$\frac{d^2 - b^2}{f^2}\bar{x}^2$	$\frac{2d\bar{x}}{af}$	
0	0	0	$\frac{2a^2b\bar{x}^2}{cg^2}$	$\frac{a^2c^2 - a^2b^2}{c^2g^2}\bar{x}^2$	$-\frac{2a\bar{x}}{cg}$	$\frac{2a^2b}{df^2}M_6$	$\frac{a^2(d^2 - b^2)}{d^2f^2}M_6$	$\frac{2a}{df}M_1$	

$$M_1 = 1 - \bar{x} \quad M_3 = \bar{x} - 2\bar{x}^2 \quad M_5 = 1 - 2\bar{x} \quad M_7 = 1 - 4\bar{x} + 3\bar{x}^2$$

$$M_2 = 3\bar{x}^2 - 2\bar{x} \quad M_4 = \bar{x} - \bar{x}^2 \quad M_6 = 1 - 2\bar{x} + \bar{x}^2 \quad M_8 = 1 - 3\bar{x} + 2\bar{x}^2$$

x, y and z.

2.4 Total Element Stiffness Matrix

Equations (20) and (34) express the matrix formulations for plane stress stiffnesses and bending stiffnesses respectively. The plane stress stiffness, derived on the basis of the theory of plane stress, indicates that displacements U and V are related only with the in-plane forces N_x and N_y . The bending stiffness, derived on the basis of the Lagrangian - Kirchhoff Plate Theory, indicates that displacements θ_x , θ_y and W are related only with actions M_y , M_x and Q_z . Thus, the total element stiffness matrix may be expressed as

$$[K] = \begin{bmatrix} K_p & 0 \\ 0 & K_b \end{bmatrix} \quad (35)$$

where

K = total element stiffness matrix

K_p = plane stress stiffness matrix

K_b = bending stiffness matrix.

However, the form of equation (35) may be improved by grouping linear and rotational displacements and the corresponding forces and moments. Displacement and action vectors for a node i of the triangular element are:

$$\{q_i\} = \begin{bmatrix} U_i \\ V_i \\ W_i \\ \theta_{xi} \\ \theta_{yi} \\ \theta_{zi} \end{bmatrix} \quad \{S_i\} = \begin{bmatrix} N_{xi} \\ N_{yi} \\ Q_{zi} \\ M_{yi} \\ M_{xi} \\ M_{zi} \end{bmatrix} . \quad (36)$$

The total element stiffness matrix conforming to equations (36) is built up from the elements of $[K_p]$ and $[K_b]$ as demonstrated in Table XII. The rotation θ_z is taken to be zero in this paper since the angle at which the finite elements meet in a smoothly curving shell is small. For structures in which the plate elements meet at a significant angle, as at the fold line in a folded plate structure, the stiffness corresponding to θ_z could have a controlling influence on the plate bending actions (21). The moment M_z is zero in the elemental system.

If an element has node points i, j and k, the total element stiffness matrix (Table XII) may be partitioned into 6x6 submatrices as

$$[K] = \begin{bmatrix} K_{ii} & K_{ij} & K_{ik} \\ K_{ji} & K_{jj} & K_{jk} \\ K_{ki} & K_{kj} & K_{kk} \end{bmatrix} . \quad (37)$$

TABLE XII
ELEMENT STIFFNESS MATRIX

N_{xi}	K_{p11}	K_{p12}	0	0	0	0	K_{p13}	K_{p14}	0	0	0	0	K_{p15}	K_{p16}	0	0	0	0	U_i
N_{yi}		K_{p22}	0	0	0	0	K_{p23}	K_{p24}	0	0	0	0	K_{p25}	K_{p26}	0	0	0	0	V_i
Q_{zi}			K_{b33}	K_{b31}	K_{b32}	0	0	0	K_{b36}	K_{b34}	K_{b35}	0	0	0	K_{b39}	K_{b37}	K_{b38}	0	W_i
M_{yi}				K_{b11}	K_{b12}	0	0	0	K_{b16}	K_{b14}	K_{b15}	0	0	0	K_{b19}	K_{b17}	K_{b18}	0	θ_{xi}
M_{xi}					K_{b22}	0	0	0	K_{b26}	K_{b24}	K_{b25}	0	0	0	K_{b29}	K_{b27}	K_{b28}	0	θ_{yi}
M_{zi}						0	0	0	0	0	0	0	0	0	0	0	0	0	θ_{zi}
N_{xj}							K_{p33}	K_{p34}	0	0	0	0	K_{p35}	K_{p36}	0	0	0	0	U_j
N_{yj}								K_{p44}	0	0	0	0	K_{p45}	K_{p46}	0	0	0	0	V_j
Q_{zj}									K_{b66}	K_{b64}	K_{b65}	0	0	0	K_{b69}	K_{b67}	K_{b68}	0	W_j
M_{yj}										K_{b44}	K_{b45}	0	0	0	K_{b49}	K_{b47}	K_{b48}	0	θ_{xj}
M_{xj}											K_{b55}	0	0	0	K_{b59}	K_{b57}	K_{b58}	0	θ_{yj}
M_{zj}												0	0	0	0	0	0	0	θ_{zj}
N_{xk}													K_{p55}	K_{p56}	0	0	0	0	U_k
N_{yk}														K_{p66}	0	0	0	0	V_k
Q_{zk}															K_{b99}	K_{b97}	K_{b98}	0	W_k
M_{yk}																K_{b77}	K_{b78}	0	θ_{xk}
M_{xk}																	K_{b88}	0	θ_{yk}
M_{zk}																		0	θ_{zk}

(SYMMETRICAL)

CHAPTER III

FORMULATION AND SOLUTION

3.1 Axes Transformation

The element stiffness matrix (Table XII) developed in Chapter II is referenced to the axes system of the element. Before the elemental stiffnesses can be combined to form the structural stiffness it is necessary to transform each elemental stiffness from its own system to one common system, referred to as the structural system. Figure 12 shows an elemental system and the structural system. Superscript "a" refers to the elemental system while "o" refers to the structural system.

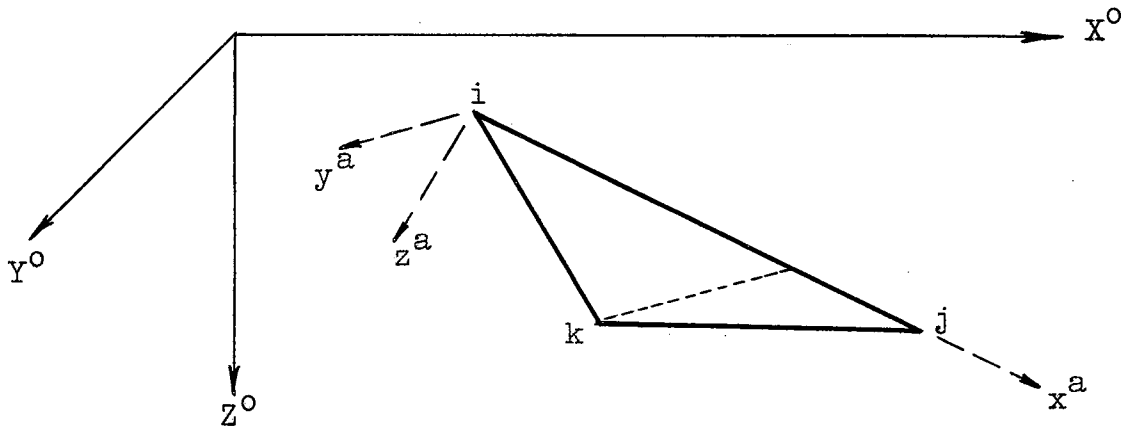


Figure 12. Axes Reference Systems

Displacements and forces are transformed from the elemental to the structural system by performing three rotations. The transformation for a node point i may be expressed as

$$\{q_i^a\} = [\Psi] \{q_i^o\} \quad (38)$$

and

$$\{S_i^a\} = [\Psi] \{S_i^o\} . \quad (39)$$

The vectors $\{q_i\}$ and $\{S_i\}$ are as in equation (36) and the transformation matrix is:

$$[\Psi] = \begin{bmatrix} \alpha_{oax} & \beta_{oax} & \gamma_{oax} & & & \\ \alpha_{oay} & \beta_{oay} & \gamma_{oay} & & & \\ \alpha_{oaz} & \beta_{oaz} & \gamma_{oaz} & & & \\ & & & 0 & & \\ & & & & \alpha_{oax} & \beta_{oax} & \gamma_{oax} \\ & & & & \alpha_{oay} & \beta_{oay} & \gamma_{oay} \\ & & & & \alpha_{oaz} & \beta_{oaz} & \gamma_{oaz} \end{bmatrix} \quad (40)$$

where

α_{oax} = cosine of angle between X^a and X^o axes

β_{oax} = cosine of angle between X^a and Y^o axes

γ_{oax} = cosine of angle between X^a and Z^o axes

•
•
•

γ_{oaz} = cosine of angle between Z^a and Z^o axes .

The element transformation matrix is constructed from equation (40) and may be expressed as

$$[\Omega] = \begin{bmatrix} \Psi & 0 & 0 \\ 0 & \Psi & 0 \\ 0 & 0 & \Psi \end{bmatrix}. \quad (41)$$

Elements of the Ψ -matrix are derived by expressing each of the elemental axes as a vector in terms of the structural system coordinates of the node points. This results in the following nine equations for the direction cosines.

$$\alpha_{oax} = \frac{x_j - x_i}{a} \quad (42a)$$

$$\beta_{oax} = \frac{y_j - y_i}{a} \quad (42b)$$

$$\gamma_{oax} = \frac{z_j - z_i}{a} \quad (42c)$$

$$\alpha_{oay} = \frac{x_k - x_i - c\alpha_{oax}}{b} \quad (42d)$$

$$\beta_{oay} = \frac{y_k - y_i - c\beta_{oax}}{b} \quad (42e)$$

$$\gamma_{oay} = \frac{z_k - z_i - c\gamma_{oax}}{b} \quad (42f)$$

$$\alpha_{oaz} = \beta_{oax} \gamma_{oay} - \beta_{oay} \gamma_{oax} \quad (42g)$$

$$\beta_{oaz} = \alpha_{oay} \gamma_{oax} - \alpha_{oax} \gamma_{oay} \quad (42h)$$

$$\gamma_{oaz} = \alpha_{oax} \beta_{oay} - \alpha_{oay} \beta_{oax} \quad (42i)$$

The element stiffness is transformed from the elemental (a) system to the structural (o) system by the following matrix operations:

$$\{S^a\} = [K^a] \{q^a\} \quad (43)$$

or

$$[\Omega] \{S^o\} = [K^a] [\Omega] \{q^o\}$$

therefore

$$\{S^o\} = [\Omega]^T [K^a] [\Omega] \{q^o\}$$

or

$$\{S^o\} = [K^o] \{q^o\} \quad (44)$$

where

$$[K^o] = [\Omega]^T [K^a] [\Omega] . \quad (45)$$

3.2 Structural Stiffness Matrix

Equation (45) expresses the stiffness of a single finite element in reference to the structural system. There are as many such matrices as there are finite elements. These are evaluated and then combined to form the structural stiffness matrix which is of size $6n \times 6n$, where n is the number of node points in the entire structure. This structural stiffness matrix, designated $[SK]$, relates the generalized displacements of each and every node to the external load vector,

$$\{F\} = [SK] \{q\} , \quad (46)$$

where $\{F\}$ is the vector of external loads, $[SK]$ is the matrix of stiffness coefficients and $\{q\}$ is the vector of

generalized nodal displacements. The superscript designating system of axes is omitted from equation (46) since the formulation requires that all loads and displacements be referenced to the structural system.

3.3 Boundary Conditions

The formulation of equation (46) allows for solution of generalized displacements $\{q\}$ only after proper constraints have been applied to render the structure stable. These constraints are applied in the form of boundary, or support, conditions.

It is in the application of boundary conditions that the finite element method has a distinct advantage over classical theory. Boundary conditions can be physically reasoned without concern for such effects as concentrated corner forces which occur in Kirchhoffian plate theory or shear forces which occur along plate edges.

Since there are six degrees of freedom at each node, there are six possible conditions of constraint at each node which may be applied singly or in any combination. For any node point i these are:

$$U_i = 0$$

$$V_i = 0$$

$$W_i = 0$$

$$\theta_{xi} = 0$$

$$\theta_{yi} = 0$$

$$\theta_{zi} = 0$$

For each rigid constraint, the corresponding row and column of the stiffness matrix is deleted and the order of the matrix is reduced by one. Therefore, if r is the number of constraints, the order of the reduced stiffness matrix is $(6n-r)$.

3.4 Skewed Boundaries

The ability to work with skewed boundaries is a necessity for analyzing arbitrarily shaped plates or shells. It is also desirable when working with regular structures which have skewed axes. Since computer storage capacity is critical in the finite element method, it is important to take full advantage of symmetry whenever possible. For example, a symmetrical umbrella shell, symmetrically loaded, may be analyzed by considering only one-half of one quadrant.

The stiffness matrix must be modified by transforming the rows and columns which correspond to node points lying on a skewed boundary. Figure 13 represents a boundary which is skewed with respect to the structural system. The angle of skew is in the X-Y plane.

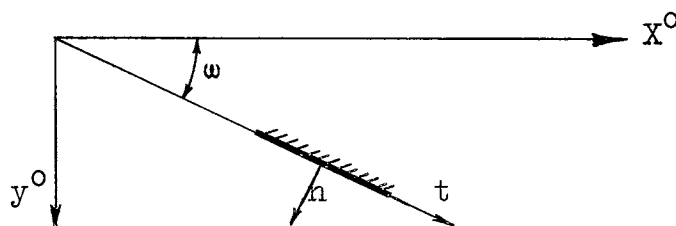


Figure 13. Skewed Boundary Axes

The relation between displacements at node i in the two systems may be expressed: (superscript "b" refers to skewed system of axes).

$$\begin{bmatrix} U_i^o \\ V_i^o \\ W_i^o \\ \theta_{xi}^o \\ \theta_{yi}^o \\ \theta_{zi}^o \end{bmatrix} = \begin{bmatrix} \cos \omega & -\sin \omega & 0 & & & \\ \sin \omega & \cos \omega & 0 & & & \\ 0 & 0 & 0 & & & \\ & & & 0 & & \\ & & & & 0 & \\ & & & & & 0 \end{bmatrix} + \begin{bmatrix} & & & & & \\ & & & & & \\ & & & & & \\ \cos \omega & -\sin \omega & 0 & & & \\ \sin \omega & \cos \omega & 0 & & & \\ 0 & 0 & 1 & & & \end{bmatrix} \begin{bmatrix} U_i^b \\ V_i^b \\ W_i^b \\ \theta_{xi}^b \\ \theta_{yi}^b \\ \theta_{zi}^b \end{bmatrix}$$

or

$$\{q_i^o\} = [\omega] \{q_i^b\} . \quad (47)$$

In a similar manner:

$$\{F_i^o\} = [\omega] \{F_i^b\} . \quad (48)$$

The stiffness matrix for a structure in which some of the nodes lie on non-skewed axes while others lie on skewed axes is a "mixed" matrix. That is to say, some of the elements are in the structural system, others are in the skew system while still others are in a structural-skew system. In the mixed matrix there are four different relations between forces and displacements.

- i) F^o related with q^o
- ii) F^o related with q^b
- iii) F^b related with q^o
- iv) F^b related with q^b

Condition (i) requires no modification in the stiffness matrix. Condition (ii) requires that all columns of $[SK]$ corresponding to a node on the skew boundary be post-multiplied by $[\omega]$. Condition (iii) requires that all rows of $[SK]$ corresponding to a node on the skew boundary be pre-multiplied by $[\omega]^T$. Condition (iv) is satisfied by the operations of (ii) and (iii). These matrix operations are conveniently carried out by working with the 6×6 submatrices which correspond to each node point. It is, of course, possible to have many different skewed boundaries in a single structure. Such would be the case for a circular plate or any irregular shaped plate or shell.

3.5 Deformations

The elemental stiffness matrices (Table XII) are transformed to the structural system and combined to form the structural stiffness matrix. This matrix is then reduced in accordance with applied boundary conditions and modified, if necessary, for skewed axes. This results in a set of $(6n-r)$ simultaneous equations which are solved to yield the deformations at each and every node point.

3.6 Stresses and Stress Resultants

Having determined the generalized displacements at each node point, stresses in the individual finite elements may be evaluated. This is accomplished by selecting from the displacement vector those values corresponding to the

three nodes of the particular element in question. These displacement values are then transformed from the structural system to the elemental system and used to build vectors $\{q_p\}$ and $\{q_b\}$. Equations (17) and (33) are substituted into equations (4) and (24) respectively to yield

$$\{\sigma_p\} = [P_p] [H_p]^{-1} [T_p] \{q_p\} \quad (49)$$

and

$$\{\sigma_b\} = [P_b] [H_b]^{-1} [T_b] \{q_b\} . \quad (50)$$

After solving equations (49) and (50), the in-plane and bending actions are evaluated from equations (2) and (22) respectively.

CHAPTER IV

APPLICATION TO HYPERBOLIC PARABOLOID SHELLS

4.1 General Procedure

The first step in applying the finite element method of analysis to a shell, or any elastic continuum, is to idealize the structure by subdividing it into an assemblage of discrete members, triangular elements in the case of doubly curved shells. There are many different ways in which this can be done and, of course, the closer the idealization is to the actual structure, the better the results.

Secondly, the elastic characteristics of the finite element are determined. This has been presented in detail in Chapter II. In this presentation matrices $[H_p]$ (Tables II and III), $[T_p]$ (Table VI), $[H_b]$ (Tables VIII and IX) and $[T_b]$ (Appendix A) are hand formulated in terms of the elastic properties and the geometry of the finite element. They are then coded in FORTRAN and an IBM 7040 Digital Computer is used to evaluate the element stiffness matrices (equations 20 and 34; and Table XII).

The third step consists of the structural analysis of the entire assemblage of elements. Details concerning axes transformation, boundary conditions and skewed axes

are presented in Chapter III. This step is carried out completely on the computer. A flow chart of the computer program is given in Appendix B.

The procedure outlined above is applied to the analysis of two hyperbolic paraboloidal shells, details of which are given in the next sections.

4.2 Edge Supported Shell

The shell shown in Figure 14 is analyzed for deformations due to a uniformly distributed vertical load of 0.3472 pounds per square inch. The middle surface of the shell is defined by the equation

$$Z = \frac{L_z XY}{L_x L_y} \quad (51)$$

The shell is supported along all four edges by diaphragms which are considered to be incapable of vertical deflections while offering no resistance to normal displacements. Elastic properties and dimensions of the shell are given in Table XIII.

The shell is subdivided into an assemblage of triangular elements as shown in planform in Figure 15. A finer grid is selected near the center of the shell anticipating this to be the region of larger deflections. Since the shell is symmetrically loaded and is also geometrically symmetrical with respect to aoc and bod (Figure 14), it can be analyzed by considering one quadrant such as cod.

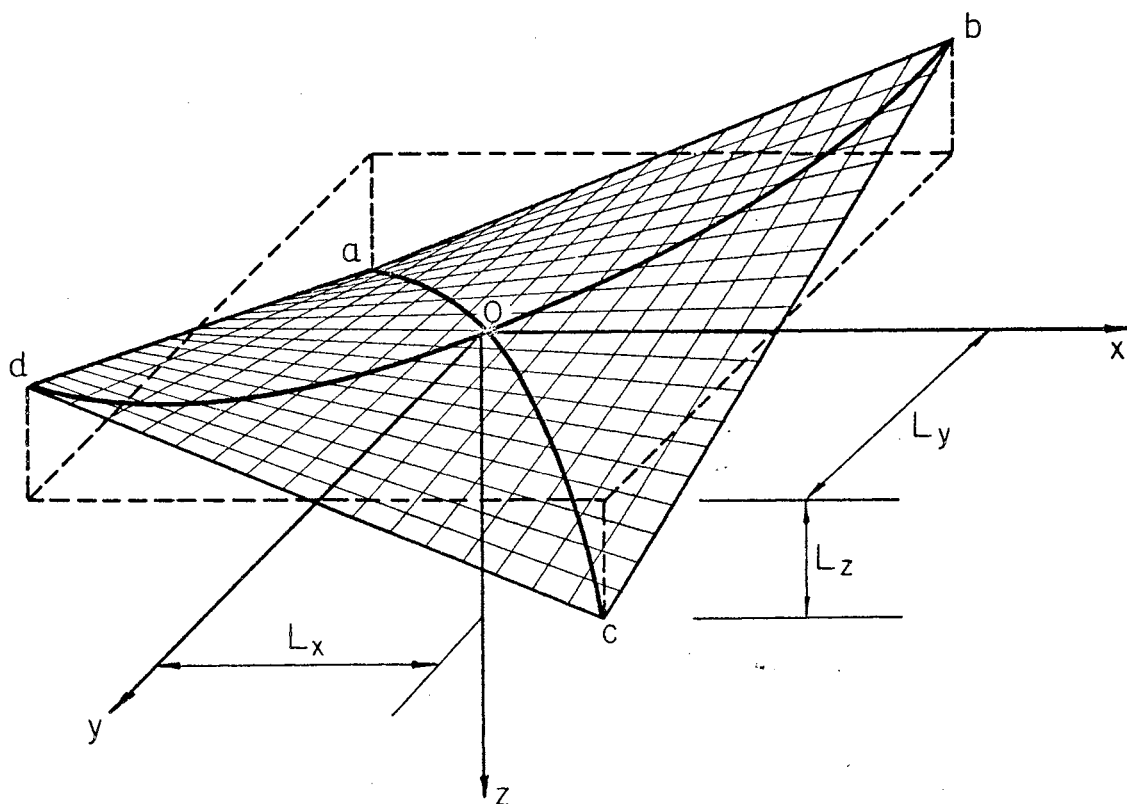


Figure 14. Edge Supported Shell

TABLE XIII

PROPERTIES OF EDGE SUPPORTED SHELL

$$L_x = 180 \text{ in.}$$

$$L_y = 180 \text{ in.}$$

$$L_z = 36 \text{ in.}$$

$$E = 3 \times 10^6 \text{ psi}$$

$$t = 2.5 \text{ in.}$$

$$\nu = 0.16$$

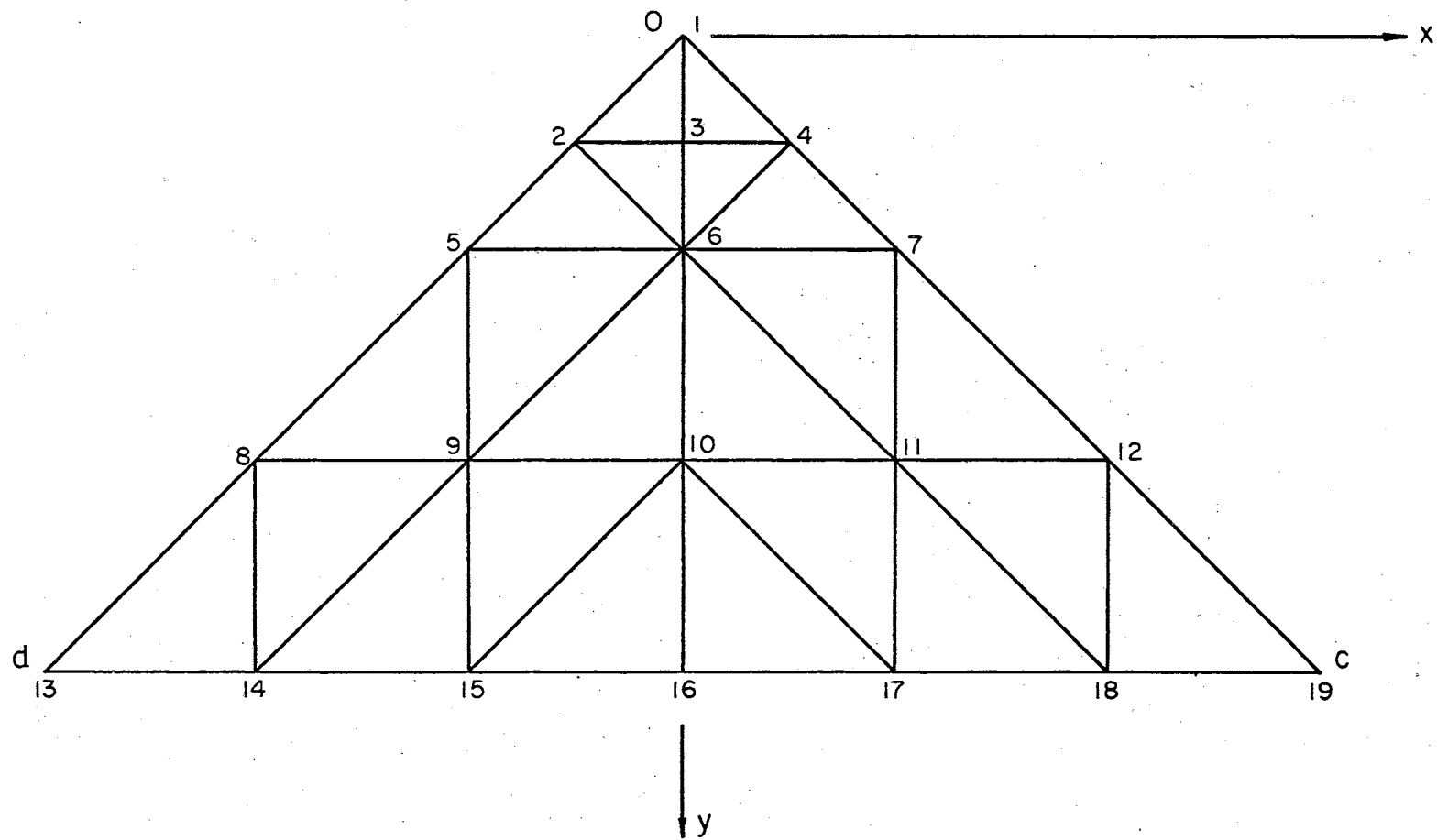


Figure 15. Finite Element Idealization of Edge Supported Shell

Deformations at the node points of the shell are listed in Table XIV while Figure 16 shows a contour plot of vertical deflections.

4.3 Inverted Umbrella Shell

The shell shown in Figure 17 is a popular form of the hyperbolic paraboloid and is known as the inverted umbrella shell. This shell is analyzed for deformations due to a uniformly distributed vertical load of 0.4861 pounds per square inch. The middle surface of the shell is defined by the equation

$$z = \frac{L_z}{L_x L_y} (L_x - x)(L_y - y) . \quad (52)$$

The shell is supported by a single column at the center and stiffened by ribs and edge beams as shown in Figure 18. The tapered rib is approximated by elements of constant thickness, each having a different thickness. Elastic properties and dimensions of the shell are given in Table XV.

The idealized shell is shown in planform in Figure 19. Due to conditions of symmetry the shell can be analyzed by considering one-half of one quadrant. Deformations at the node points are listed in Table XVI and a contour plot of the vertical deflections is shown in Figure 20.

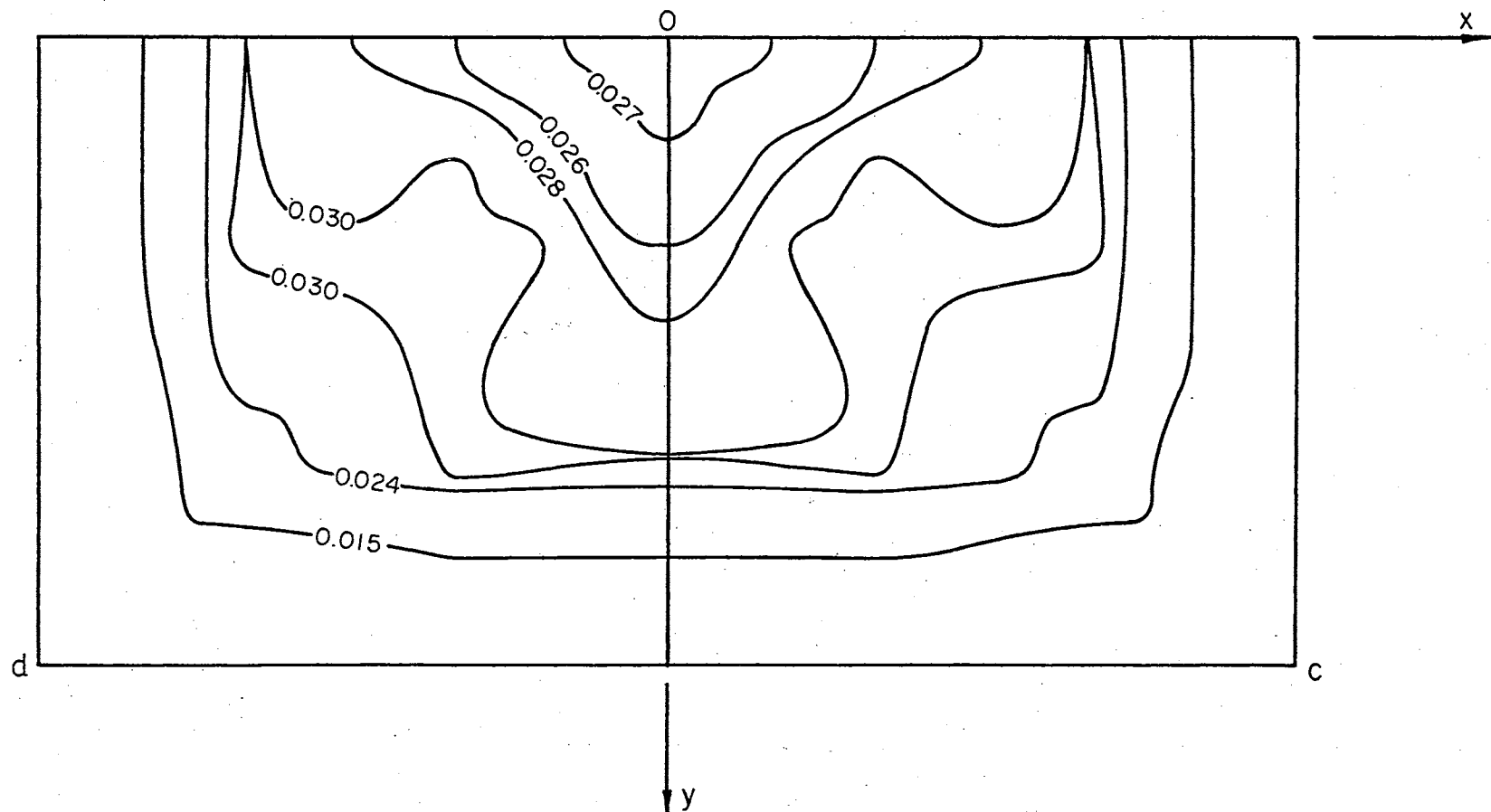


Figure 16. Vertical Deflections For Edge Supported Shell

TABLE XIV
NODE POINT DEFORMATIONS FOR EDGE SUPPORTED SHELL

NODE POINT	U (in.)	V (in.)	W (in.)	θ_x (rad.)	θ_y (rad.)	θ_z (rad.)
1	0.000000	0.000000	0.028153	0.000000	0.000000	0.000000
2	-0.000710	0.000710	0.025991	0.000001	0.000001	0.000000
3	-0.000700	-0.000000	0.026559	0.000163	-0.000000	-0.007813
4	-0.000710	-0.000710	0.025991	0.000001	-0.000001	0.000000
5	-0.001780	0.001780	0.033467	0.000152	0.000152	0.000000
6	-0.001302	-0.000000	0.026027	0.000089	-0.000000	0.000414
7	-0.001780	-0.001780	0.033467	0.000152	-0.000152	0.000000
8	-0.002086	0.002086	0.022003	-0.000299	-0.000299	0.000000
9	-0.003140	0.001625	0.030958	-0.000243	-0.000089	-0.000606
10	-0.002936	0.000000	0.029764	0.000118	-0.000000	-0.002285
11	-0.003140	-0.001625	0.030958	-0.000243	0.000089	-0.000606
12	-0.002086	-0.002086	0.022003	-0.000299	0.000299	0.000000
13	0.000000	0.000000	0.000000	0.000000	0.000000	0.000000
14	0.000000	-0.000732	0.000000	-0.000440	0.000000	-0.000009
15	0.000000	-0.000395	0.000000	-0.000691	0.000000	0.000211
16	0.000000	0.000000	0.000000	0.006675	0.000000	-0.036501
17	0.000000	0.000395	0.000000	-0.000691	0.000000	0.000211
18	0.000000	0.000732	0.000000	-0.000440	0.000000	-0.000009
19	0.000000	0.000000	0.000000	0.000000	0.000000	0.000000

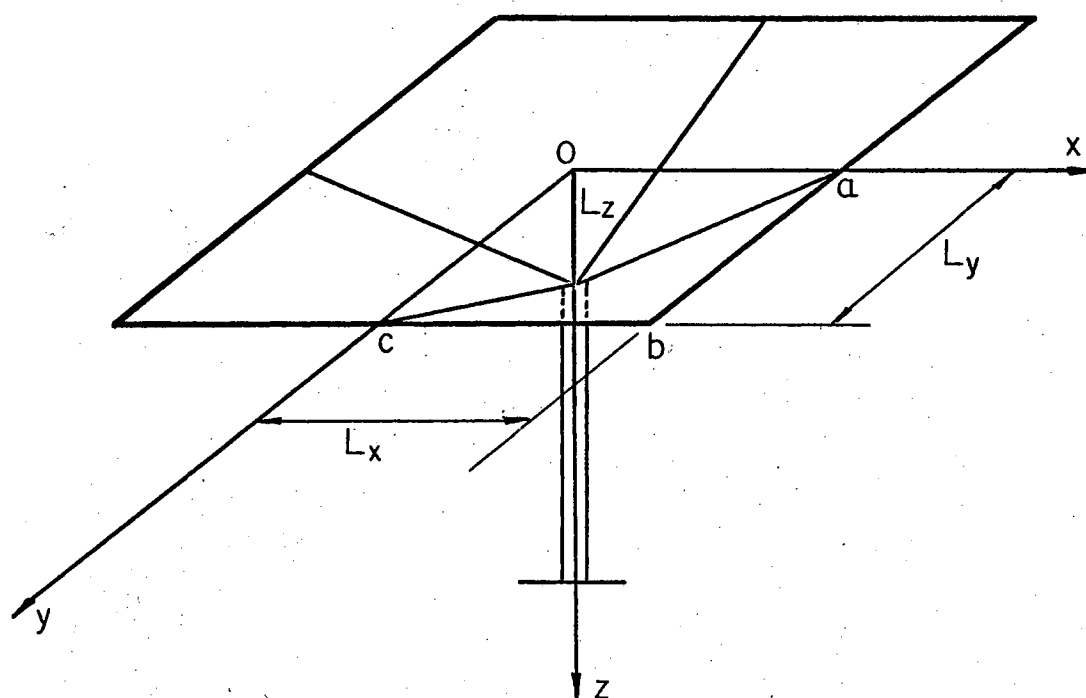


Figure 17. Inverted Umbrella Shell

TABLE XV

PROPERTIES OF INVERTED UMBRELLA SHELL

$$L_x = 144 \text{ in.}$$

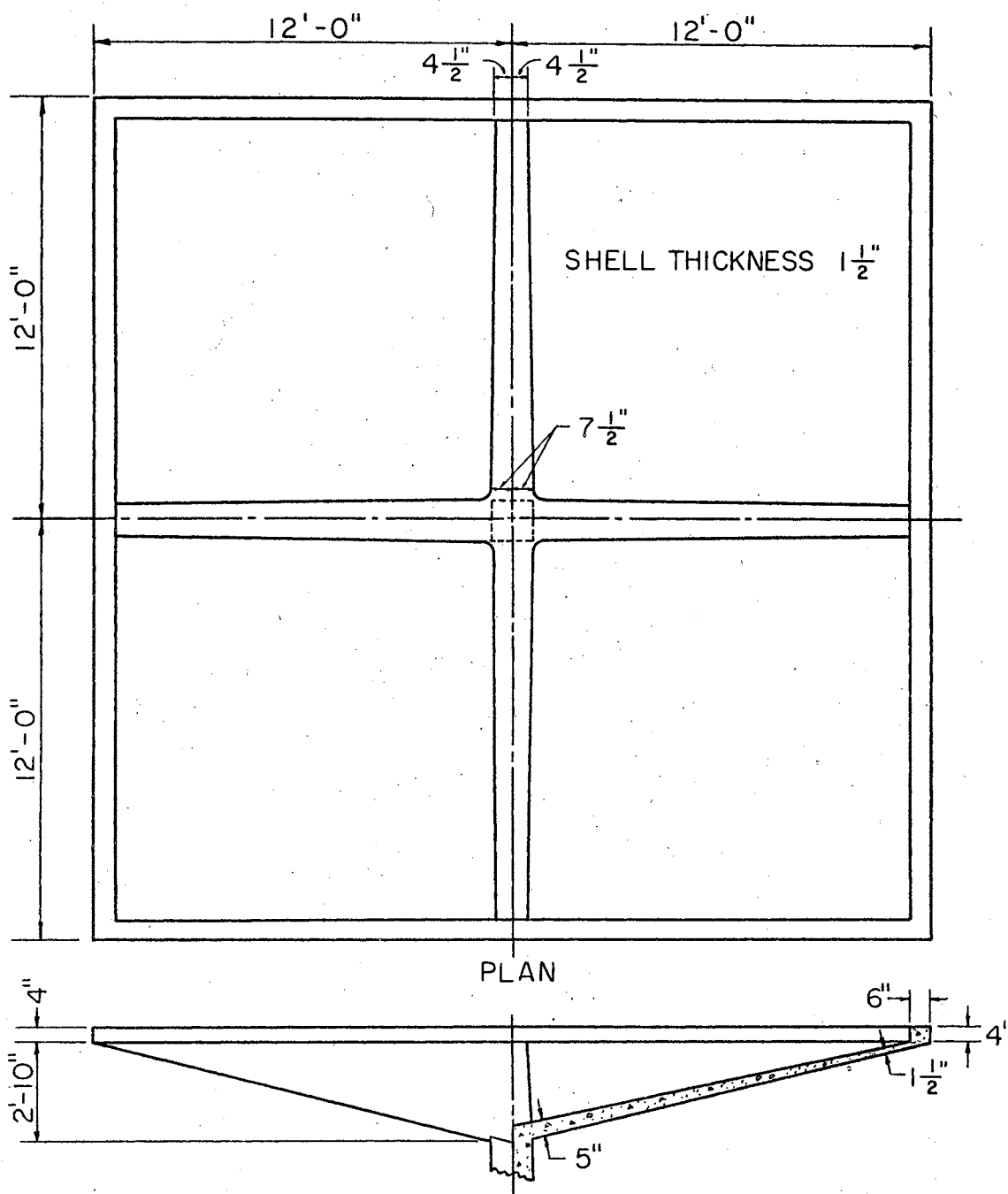
$$L_y = 144 \text{ in.}$$

$$L_z = 36 \text{ in.}$$

$$E = 3.85 \times 10^6 \text{ psi}$$

$$t = 1.5 \text{ in.}$$

$$\nu = 0.10$$



HALF ELEVATION AND HALF SECTION THROUGH C.L.

Figure 18. Rib and Edge Beams For Inverted Umbrella Shell

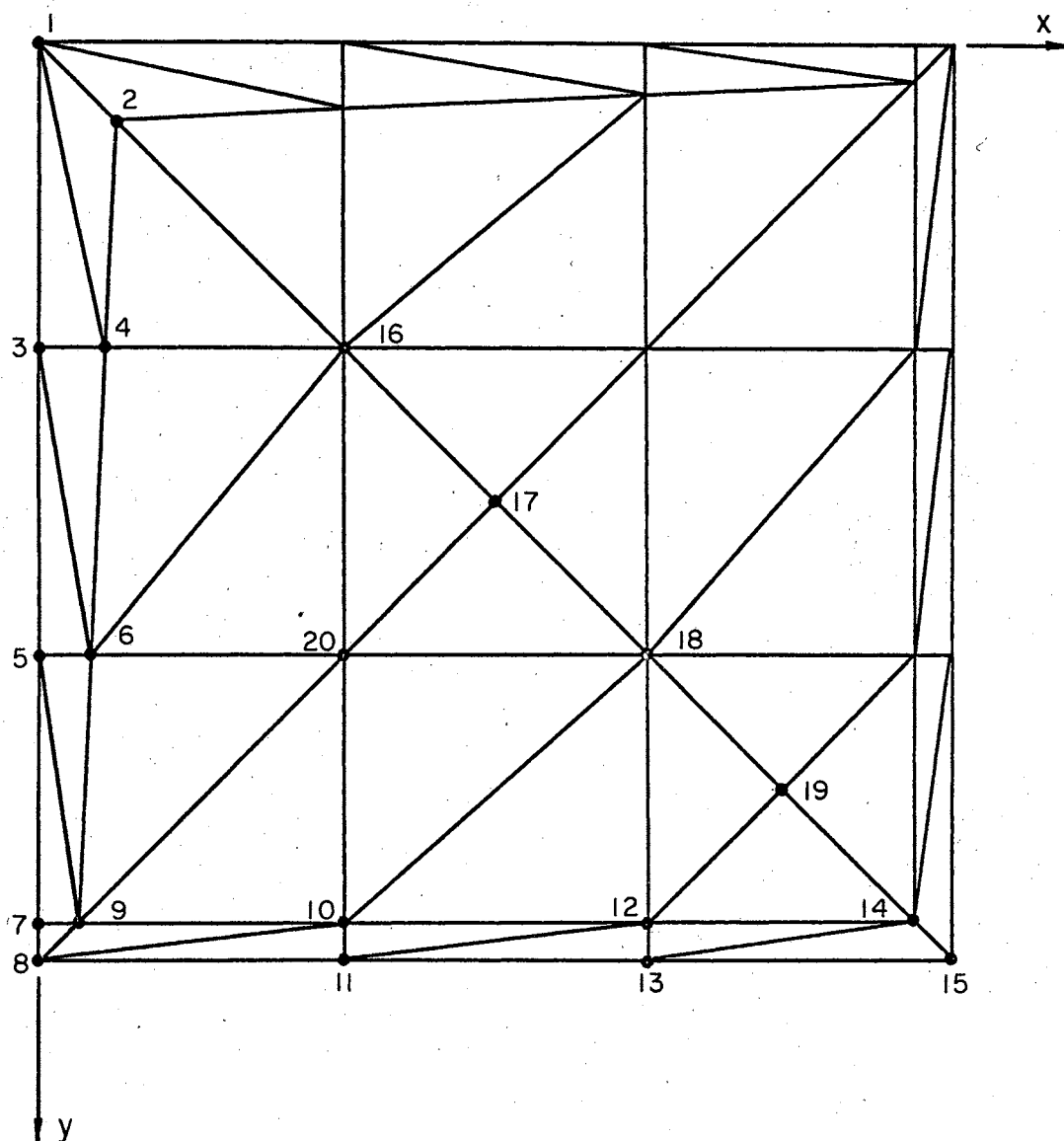


Figure 19. Finite Element Idealization of Inverted Umbrella Shell

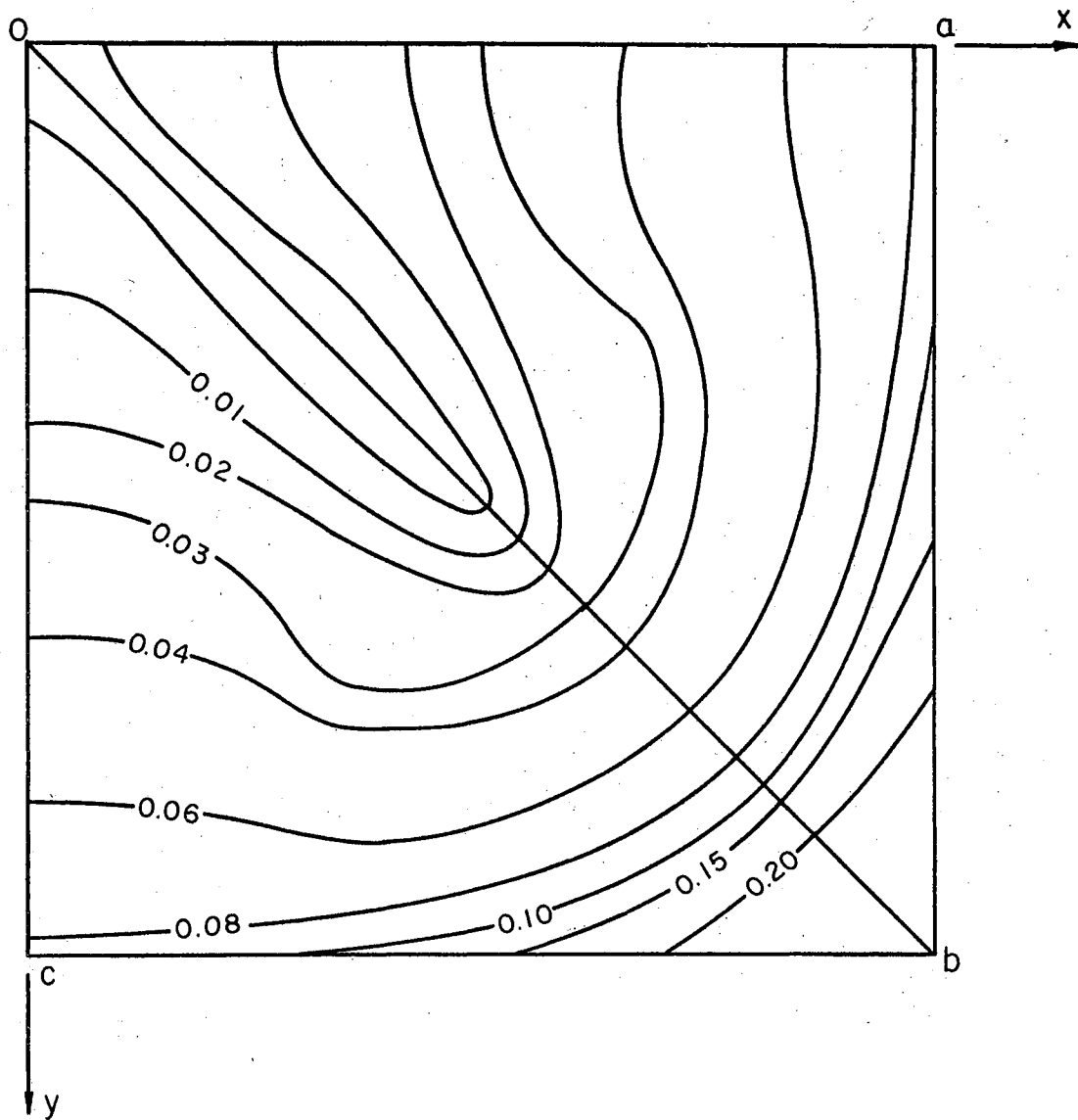


Figure 20. Vertical Deflections For Inverted Umbrella Shell

TABLE XVI

NODE POINT DEFORMATIONS FOR INVERTED UMBRELLA SHELL

NODE POINT	U (in.)	V (in.)	W (in.)	θ_x (rad.)	θ_y (rad.)	θ_z (rad.)
1	0.000000	0.000000	0.000000	0.000000	0.000000	0.000000
2	0.000000	0.000000	0.000000	0.000000	0.000000	0.000000
3	0.000000	-0.000024	0.013445	0.000436	0.000000	0.000000
4	0.000010	0.000325	0.013332	-0.000311	-0.001072	-0.004526
5	0.000000	0.004634	0.041636	0.000575	0.000000	0.000000
6	0.000009	0.004886	0.041539	0.000487	-0.000221	-0.001061
7	0.000000	0.014046	0.080419	0.001574	0.000000	0.000000
8	0.000000	0.016827	0.089709	0.001538	0.000000	0.000000
9	0.000052	0.013983	0.080457	0.001584	0.000145	0.000630
10	0.003766	0.011992	0.095786	0.001969	-0.000712	-0.000078
11	0.004963	0.013923	0.107720	0.001980	-0.000227	0.003232
12	0.006772	0.008703	0.152754	0.002603	-0.002361	-0.003781
13	0.008003	0.009949	0.168241	0.002608	-0.002190	-0.001030
14	0.008957	0.008957	0.258872	0.002806	-0.002806	0.000000
15	0.009129	0.009129	0.292626	0.002851	-0.002351	0.000000
16	-0.003206	-0.003206	-0.004403	-0.000436	0.000436	0.000000
17	-0.003839	-0.003839	-0.002405	0.000337	-0.000337	0.000000
18	0.000029	0.000029	0.040601	0.001751	-0.001751	0.000000
19	0.006548	0.006548	0.158948	0.002888	-0.002888	0.000000
20	-0.000999	0.001422	0.028810	0.001202	0.000393	-0.001361

CHAPTER V

SUMMARY AND CONCLUSIONS

5.1 Summary

A stiffness method for the analysis of shells of double curvature is presented in this dissertation. The shell is idealized as an assemblage of plane triangular shaped elements connected together at their node points. Equilibrium is established within each element and at the node points and compatibility of deformations is satisfied along the line separating adjacent elements. The development consists mainly of formulating the elemental stiffness matrices which are derived on the basis of an assumed stress function. Final solution is effected by the use of a digital computer.

Two hyperbolic paraboloid shells, one supported along all four edges and the other supported by a central column, are analyzed for deformations to demonstrate the method.

5.2 Discussion of Results

The number of doubly curved shells for which solutions are reported in the literature is very limited. The shells selected as examples in this paper have been analyzed by

other methods and the results, to a certain extent, are available for comparison.

A solution by application of Bongard's simplified equations for the edge supported shell shown in Figure 14 is reported by Chetty and Tottenham (6). They list vertical deflections for a section along the y-axis. Figure 21 shows a comparison of deflections obtained by the two methods. There is considerable variation in the deflection pattern although maximum values, 0.038 inches as opposed to 0.033 inches, compare quite favorably.

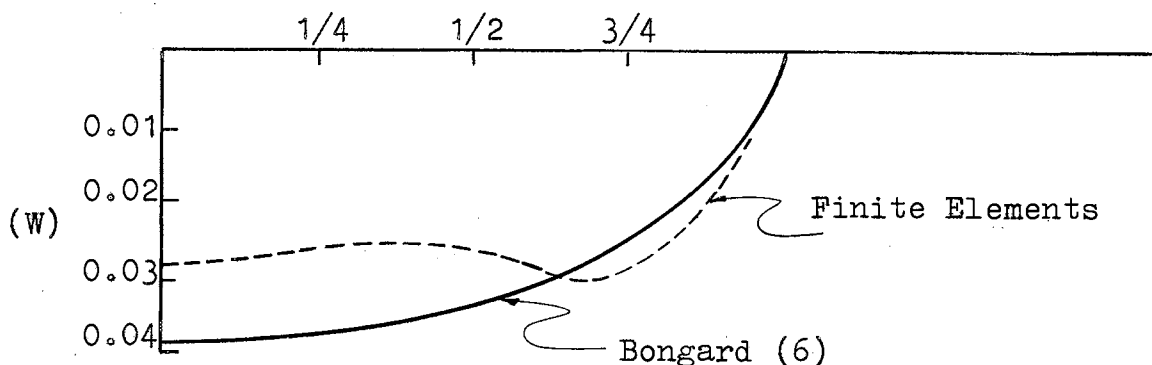


Figure 21. Vertical Deflection Profile Along Y-Axis of Edge Supported Shell

Bending stress resultants are calculated in accordance with the procedure discussed in section 3.6. Discontinuities in the bending moments do occur according to which of the contiguous elements is used in the calculation at a particular node point. As indicated by equations (49) and (50) the stresses, and therefore the stress resultants, are

a function of the generalized displacements at all three nodes of an element. Thus, it is expected that there should be a certain amount of discontinuity in the moment values. The magnitudes of the discontinuities are dependent upon the element size and orientation relative to other elements joining at the node point. Table XVII lists values of M_y at several node points as calculated from different elements to illustrate the discrepancies.

TABLE XVII
BENDING MOMENTS FOR SHELL OF FIGURE 14

<u>Node Point</u>	<u>Moment M_y (In-Lb/In)</u>		
3	-22.50	-22.50	- 2.08
6	27.93	12.68	21.24
10	-19.24	-25.27	-20.08
11	-11.67	-28.55	-11.57
12	-45.17	-28.28	-19.87

The deformations calculated for the inverted umbrella shell (Figure 17) are comparable with experimental results obtained in a laboratory test and reported by the Portland Cement Association (22). The vertical deflection contours calculated in this dissertation are in very close agreement with the experimental results. There is a difference in the magnitude of the deflections as the experimental results include the effects of creep and plastic flow of the concrete. Discontinuities of the stress resultants, similar to those

discussed in the previous paragraph, also occurred for the inverted umbrella shell.

5.3 Conclusions and Possible Extensions

The presentation provides a general solution for determining deformations in shells of double curvature. The method applies equally well to other plate and shell structures provided that the middle surface is either flat or smoothly curved. Based on a limited number of applications, it is concluded that the method yields accurate deformations. It is believed that this is the first general solution for shells in which the stiffnesses of ribs and edge beams have been incorporated directly in the analysis.

The method does not admit to accurate results as far as internal forces and moments are concerned. The orientation of the elements within the structure appears to have a significant influence on the results. A considerable amount of work remains to be done in this area and perhaps a method for predicting an optimum orientation can be derived.

The use of curved elements to represent shell surfaces is almost an untouched field and holds promise as a better way of idealizing complicated shapes. The curved element itself could be idealized as an assemblage of triangular elements and its elastic characteristics evaluated by the method of this dissertation.

BIBLIOGRAPHY

- (1) Candela, Felix. "Understanding the Hyperbolic Paraboloid." Architectural Record. (July and August, 1958).
- (2) Aimond, F. "Treatise on Statics of Parabolic Hyperboloidal Shells not Stiff in Bending." Internat. Assoc. for Bridge and Structural Engineering Publications, Vol. 4, (1936) 1-112.
- (3) Vlasov, V. S. Allgemeine Schalentheorie und Ihre Anwendung in der Technik. Akademie-Verlag, Berlin. (1958).
- (4) Margurre, K. "Zur Theorie der Gekrummten Platte Geober Formanderung." Proc. 5th Internat. Congress of Applied Mech. (1938) 93.
- (5) Bongard, W. "Zur Theorie and Berechnung Von Schalen-tragwerken in Form Gleichscitiger Hyperbolischer Paraboloid." Bautechnik-Archiv. Vol. 15, (1959).
- (6) Chetty, S. M. K., and H. Tottenham. "Investigation Into the Bending Analysis of Hyperbolic Paraboloid Shells." Indian Concrete Jour. (July, 1964) 248-258.
- (7) Hrennikoff, A. "Solution of Problems by the Framework Method." Jour. Applied Mech. Vol. 8. (Dec. 1941).
- (8) Levy, S. "Computation of Influence Coefficients for Aircraft Structures With Discontinuities and Sweepback." Jour. Aero. Sci. Vol. 14, No. 10. (Oct., 1947) 547.
- (9) Benscoter, S. and R. MacNeal. "Equivalent Plate Theory for a Straight Multicell Wing." NACA TN 2786. (1952).
- (10) Levy, S. "Structural Analysis and Influence Coefficients for Delta Wings." Jour. Aero. Sci. Vol. 20, No. 7. (July, 1953) 449.

- (11) Turner, M. J., R. W. Clough, H. O. Martin, and L. J. Topp. "Stiffness and Deflection Analysis of Complex Structures." Jour. Aero. Sci. Vol. 23, No. 9. (Sept., 1956).
- (12) Clough, R. W. "The Finite Element Method in Plane Stress Analysis." A.S.C.E. Second Conf. on Elec. Comp. (Sept., 1960). 345-377.
- (13) Melosh, R. J. "A Stiffness Matrix for the Analysis of Thin Plates in Bending." Jour. Aero. Sci. Vol. 28. (Jan., 1961). 34-43.
- (14) Melosh, R. J. "Basis for Derivation of Matrices for the Direct Stiffness Method." Amer. Inst. Aero. Astro. Jour. Vol. 1, No. 7. (July, 1963) 1613-1637.
- (15) Zienkiewicz, O. C., and Y. K. Cheung. "Finite Element Method of Analysis for Arch Dam Shells and Comparison With Finite Difference Procedures." Intern. Symp. Theory of Arch Dams. Southampton Univ. (1964).
- (16) Zienkiewicz, O. C., and Y. K. Cheung. "The Finite Element Method for Analysis of Elastic Isotropic and Orthotropic Slabs." Proc. Instn. Civil Engrs. Vol. 28. (Aug., 1964). 471-488.
- (17) Zienkiewicz, O. C., and Y. K. Cheung. (Discussion). "The Finite Element Method for Analysis of Elastic Isotropic and Orthotropic Slabs." Proc. Instn. Civil Engrs. Vol. 33. (Feb., 1966). 322-335.
- (18) Pian, T. H. H. "Derivation of Element Stiffness Matrices by Assumed Stress Distributions." Amer. Inst. Aero. Astro. Jour. Vol. 2. (1964) 1333-1336.
- (19) Severn, R. T., and P. R. Taylor. "The Finite Element Method for Flexure of Slabs When Stress Distributions Are Assumed." Proc. Instn. Civil Engrs. Vol. 34. (June, 1966). 153-170.
- (20) Zienkiewicz, O. C., and G. S. Holister. Stress Analysis. John Wiley and Sons. (1965).
- (21) Clough, R. W., and J. L. Tocher. "Analysis of Thin Arch Dams By The Finite Element Method." Intern. Symp. Theory of Arch Dams. Southampton Univ. (1964). 107-121.

- (22) Yu, C. W., and L. B. Kriz. Tests of A Hyperbolic Paraboloid Reinforced Concrete Shell. Portland Cement Association. Bulletin D-81.

APPENDIX A

MATRIX $[T_b]$

The general nature of the geometrical shape of the finite element requires that many of the elements in matrix T_b be lengthy expressions. Therefore, rather than presenting T_b in matrix form it is more convenient to list the individual elements.

$$T_{1,1} = \frac{b^2 c}{2g^2}$$

$$T_{1,2} = -\frac{b^3}{2g^2}$$

$$T_{1,3} = -\frac{bc}{g^2}$$

$$T_{1,4} = \frac{b^2 d}{2f^2}$$

$$T_{1,5} = \frac{b^3}{2f^2}$$

$$T_{1,6} = -\frac{bd}{f^2}$$

$$T_{1,7} = \frac{b^2 c}{2g^2} + \frac{b^2 d}{2f^2}$$

$$T_{1,8} = -\frac{b^3}{2g^2} + \frac{b^3}{2f^2}$$

$$T_{1,9} = \frac{bc}{g^2} + \frac{bd}{f^2}$$

$$T_{2,1} = \frac{b^2}{12ag^2} [4c^2 + b^2]$$

$$T_{2,2} = \frac{bc}{12ag^2} [2c^2 - b^2]$$

$$T_{2,3} = -\frac{b}{2ag^2} [b^2 + 2c^2]$$

$$T_{2,4} = \frac{b^2}{12af^2} [6cd + 2d^2 - b^2]$$

$$T_{2,5} = \frac{b}{12af^2} [6b^2c + 5b^2d + 2d^3]$$

$$T_{2,6} = \frac{b}{2af^2} [b^2 - 2cd]$$

$$T_{2,7} = \frac{b^2c^2}{4ag^2} + \frac{b^2d}{4af^2} [2c + d]$$

$$T_{2,8} = \frac{bc}{12ag^2} [-5b^2 - 2c^2] + \frac{b}{12af^2} [6b^2c + b^2d - 2d^3]$$

$$T_{2,9} = \frac{bc^2}{2ag^2} + \frac{bd}{2af^2} [2c + d]$$

$$T_{3,1} = \frac{b^2c}{4g^2}$$

$$T_{3,2} = \frac{b}{12g^2} [c^2 - 2b^2]$$

$$T_{3,3} = -\frac{bc}{2g^2}$$

$$T_{3,4} = \frac{b^2 d}{4f^2}$$

$$T_{3,5} = \frac{b}{12f^2} [2b^2 - d^2]$$

$$T_{3,6} = -\frac{bd}{2f^2}$$

$$T_{3,7} = \frac{b^2 c}{4g^2} + \frac{b^2 d}{4f^2}$$

$$T_{3,8} = \frac{b}{12g^2} [-4b^2 - c^2] + \frac{b}{12f^2} [4b^2 + d^2]$$

$$T_{3,9} = \frac{bc}{2g^2} + \frac{bd}{2f^2}$$

$$T_{4,1} = \frac{9b^2 c^3}{20a^2 g^2}$$

$$T_{4,2} = \frac{bc^2}{20a^2 g^2} [4c^2 - 5b^2]$$

$$T_{4,3} = -\frac{9bc^3}{10a^2 g^2}$$

$$T_{4,4} = \frac{b^2 d}{20a^2 f^2} [10c^2 - d^2]$$

$$T_{4,5} = \frac{b}{60a^2 f^2} [30b^2 c^2 + 20b^2 cd + 5b^2 d^2 + 20cd^3 + 8d^4]$$

$$T_{4,6} = \frac{b}{10a^2 f^2} [d^3 - 10c^2 d]$$

$$T_{4,7} = \frac{9b^2 c^3}{20a^2 g^2} + \frac{b^2 d}{20a^2 f^2} [10c^2 - d^2]$$

$$T_{4,8} = \frac{bc^2}{20a^2g^2} [-15b^2 - 6c^2] + \frac{b}{60a^2f^2} [30b^2c^2 - 20b^2cd - 5b^2d^2 - 20cd^3 - 2d^4]$$

$$T_{4,9} = \frac{bc}{10a^2g^2} [-10b^2 - c^2] + \frac{b}{10a^2f^2} [10c^2d + 10cd^2 + 10b^2c - d^3]$$

$$T_{5,1} = \frac{b^2}{60ag^2} [11c^2 + 2b^2]$$

$$T_{5,2} = \frac{bc}{20ag^2} [2c^2 - b^2]$$

$$T_{5,3} = \frac{b}{20ag^2} [-3b^2 - 9c^2]$$

$$T_{5,4} = \frac{b^2}{60af^2} [15cd + 4d^2 - 2b^2]$$

$$T_{5,5} = \frac{b}{60af^2} [10b^2c + 7b^2d - 5cd^2 + d^3]$$

$$T_{5,6} = \frac{b}{20af^2} [3b^2 - 10cd - d^2]$$

$$T_{5,7} = \frac{b^2}{20ag^2} [2c^2 - b^2] + \frac{b^2}{20af^2} [5cd + 3d^2 + b^2]$$

$$T_{5,8} = \frac{bc}{20ag^2} [-6b^2 - 3c^2] + \frac{b}{60af^2} [20b^2c + 2b^2d + 5cd^2 - 4d^3]$$

$$T_{5,9} = \frac{b}{20ag^2} [-7b^2 - c^2] + \frac{b}{20af^2} [10cd + 11d^2 + 7b^2]$$

$$T_{6,1} = \frac{3b^2c}{20g^2}$$

$$T_{6,2} = \frac{b}{60g^2} [4c^2 - 5b^2]$$

$$T_{6,3} = -\frac{3bc}{10g^2}$$

$$T_{6,4} = \frac{3b^2d}{20f^2}$$

$$T_{6,5} = \frac{b}{60f^2} [5b^2 - 4d^2]$$

$$T_{6,6} = -\frac{3bd}{10f^2}$$

$$T_{6,7} = \frac{3b^2c}{20g^2} + \frac{3b^2d}{20f^2}$$

$$T_{6,8} = \frac{b}{20g^2} [-5b^2 - 2c^2] + \frac{b}{20f^2} [5b^2 + 2d^2]$$

$$T_{6,9} = \frac{3bc}{10g^2} + \frac{3bd}{10f^2}$$

$$T_{7,1} = -\frac{a}{2} + \frac{c^3}{2g^2}$$

$$T_{7,2} = -\frac{bc^2}{2g^2}$$

$$T_{7,3} = \frac{bc}{g^2}$$

$$T_{7,4} = -\frac{a}{2} + \frac{d^3}{2f^2}$$

$$T_{7,5} = \frac{bd^2}{2f^2}$$

$$T_{7,6} = \frac{bd}{f^2}$$

$$T_{7,7} = \frac{c^3}{2g^2} + \frac{d^3}{2f^2}$$

$$T_{7,8} = -\frac{bc^2}{2g^2} + \frac{bd^2}{2f^2}$$

$$T_{7,9} = -\frac{bc}{g^2} - \frac{bd}{f^2}$$

$$T_{8,1} = -\frac{a}{6} + \frac{c^2}{12ag^2} [2c^2 - b^2]$$

$$T_{8,2} = -\frac{bc^3}{4ag^2}$$

$$T_{8,3} = \frac{bc^2}{2ag^2}$$

$$T_{8,4} = -\frac{a}{3} + \frac{d^2}{12af^2} [6cd + 4d^2 + b^2]$$

$$T_{8,5} = \frac{bd^2}{4af^2} [2c + d]$$

$$T_{8,6} = \frac{bd}{2af^2} [2c + d]$$

$$T_{8,7} = \frac{c^2}{12ag^2} [4c^2 + b^2] + \frac{d^2}{12af^2} [6cd + 2d^2 - b^2]$$

$$T_{8,8} = -\frac{bc^3}{4ag^2} + \frac{bd^2}{4af^2} [2c + d]$$

$$T_{8,9} = -\frac{bc^2}{2ag^2} - \frac{bd}{2af^2} [2c + d]$$

$$T_{9,1} = \frac{c}{12g^2} [c^2 - 2b^2]$$

$$T_{9,2} = \frac{1}{12b} [a^2 - c^2] - \frac{bc^2}{4g^2}$$

$$T_{9,3} = -\frac{d}{2b} + \frac{bc}{2g^2}$$

$$T_{9,4} = \frac{d}{12f^2} [d^2 - 2b^2]$$

$$T_{9,5} = \frac{1}{12b} [d^2 - a^2] + \frac{bd^2}{4f^2}$$

$$T_{9,6} = -\frac{c}{2b} + \frac{bd}{2f^2}$$

$$T_{9,7} = \frac{c}{12g^2} [2b^2 + 5c^2] + \frac{d}{12f^2} [2b^2 + 5d^2]$$

$$T_{9,8} = -\frac{bc^2}{4g^2} + \frac{bd^2}{4f^2} + \frac{1}{12b} [c^2 - d^2]$$

$$T_{9,9} = \frac{a}{2b} - \frac{bc}{2g^2} - \frac{bd}{2f^2}$$

$$T_{10,1} = -\frac{a}{12} + \frac{c^3}{60a^2g^2} [5c^2 - 4b^2]$$

$$T_{10,2} = -\frac{3bc^4}{20a^2g^2}$$

$$T_{10,3} = \frac{3bc^3}{10a^2g^2}$$

$$T_{10,4} = -\frac{a}{4} + \frac{d^2}{60a^2f^2} [30c^2d + 40cd^2 + 15d^3 + 10b^2c + 6b^2d]$$

$$T_{10,5} = \frac{bd^2}{20a_f^2} [10c^2 + 10cd + 3d^2]$$

$$T_{10,6} = \frac{bd}{20a_f^2} [20c^2 + 20cd + 6d^2]$$

$$T_{10,7} = \frac{c^3}{20a_g^2} [5c^2 + 2b^2] + \frac{d^2}{60a_f^2} [30c^2d + 20cd^2 + 5d^3 - 10b^2c - 4b^2d]$$

$$T_{10,8} = -\frac{3bc^4}{20a_g^2} + \frac{bd^2}{20a_f^2} [10c^2 + 10cd + 3d^2]$$

$$T_{10,9} = -\frac{3bc^3}{10a_g^2} - \frac{bd}{10a_f^2} [10c^2 + 10cd + 3d^2]$$

$$T_{11,1} = \frac{c^2}{20a_g^2} [c^2 - 2b^2]$$

$$T_{11,2} = \frac{1}{60abg^2} [2a^3g^2 - 2c^3g^2 - 9b^2c^3]$$

$$T_{11,3} = \frac{9}{60abg^2} [-a^2g^2 + c^2g^2 + 2b^2c^2]$$

$$T_{11,4} = \frac{d}{60af^2} [5cd^2 - 10b^2c - 4b^2d + 2d^3]$$

$$T_{11,5} = \frac{1}{60ab} [-3a^3 + 5cd^2 + 3d^3] + \frac{bd}{20af^2} [5cd + 2d^2]$$

$$T_{11,6} = \frac{c}{20ab} [-7c - 4d] + \frac{bd}{20af^2} [10c + 4d]$$

$$T_{11,7} = \frac{3c^2}{20ag^2} [b^2 + 2c^2] + \frac{d}{60af^2} [25cd^2 + 10b^2c + b^2d + 7d^3]$$

$$T_{11,8} = \frac{c^3}{20abg^2} [c^2 - 2b^2] + \frac{d^2}{60abf^2} [10b^2c + 4b^2d - 5cd^2 - 2d^3]$$

$$T_{11,9} = \frac{c^2}{20abg^2} [b^2 + 7c^2] + \frac{d^2}{20abf^2} [-b^2 + 10cd + 3d^2]$$

$$T_{12,1} = \frac{c}{60g^2} [15c^2 - 12b^2]$$

$$T_{12,2} = -\frac{9bc^2}{20g^2}$$

$$T_{12,3} = \frac{9bc}{10g^2}$$

$$T_{12,4} = \frac{1}{60f^2} [-20cd^2 + 10b^2c - 2b^2d - 5d^3]$$

$$T_{12,5} = \frac{b}{60f^2} [-30cd - 3d^2]$$

$$T_{12,6} = \frac{b}{10f^2} [-10c - d]$$

$$T_{12,7} = \frac{c}{20g^2} [15c^2 + 6b^2] + \frac{1}{60f^2} [5d^3 - 40cd^2 - 10b^2c + 8b^2d]$$

$$T_{12,8} = -\frac{9bc^2}{20g^2} - \frac{3bd}{60f^2} [d + 10c]$$

$$T_{12,9} = \frac{c}{10bg^2} [b^2 + 10c^2] + \frac{d}{10bfg^2} [b^2 - 10cd]$$

$$T_{13,1} = -\frac{bc^2}{g^2}$$

$$T_{13,2} = \frac{b^2c}{g^2}$$

$$T_{13,3} = -\frac{2b^2}{g^2}$$

$$T_{13,4} = \frac{bd^2}{f^2}$$

$$T_{13,5} = \frac{b^2d}{f^2}$$

$$T_{13,6} = \frac{2b^2}{f^2}$$

$$T_{13,7} = -\frac{bc^2}{g^2} + \frac{bd^2}{f^2}$$

$$T_{13,8} = \frac{b^2c}{g^2} + \frac{b^2d}{f^2}$$

$$T_{13,9} = \frac{1}{g^2} [b^2 - c^2] + \frac{1}{f^2} [d^2 - b^2]$$

$$T_{14,1} = -\frac{bc^3}{2ag^2}$$

$$T_{14,2} = \frac{a}{6} + \frac{c^2}{12ag^2} [4b^2 - 2c^2]$$

$$T_{14,3} = \frac{c^3}{ag^2} - 1$$

$$T_{14,4} = \frac{bd^2}{2af^2} [2c + d]$$

$$T_{14,5} = -\frac{a}{6} + \frac{d}{6af^2} [6b^2c + 4b^2d + d^3]$$

$$T_{14,6} = \frac{1}{af^2} [b^2a - cd^2]$$

$$T_{14,7} = -\frac{bc^3}{2ag^2} + \frac{bd^2}{2af^2} [2c + d]$$

$$T_{14,8} = \frac{c^2}{6ag^2} [4b^2 + c^2] + \frac{d}{6af^2} [6b^2c + 2b^2d - d^3]$$

$$T_{14,9} = \frac{b^2c}{ag^2} + \frac{1}{af^2} [cd^2 - b^2c + d^3]$$

$$T_{15,1} = \frac{b}{6g^2} [b^2 - 2c^2]$$

$$T_{15,2} = \frac{b^2c}{2g^2}$$

$$T_{15,3} = -\frac{b^2}{g^2}$$

$$T_{15,4} = \frac{b}{6f^2} [2d^2 - b^2]$$

$$T_{15,5} = \frac{b^2d}{2f^2}$$

$$T_{15,6} = \frac{b^2}{f^2}$$

$$T_{15,7} = \frac{b}{6g^2} [-b^2 - 4c^2] + \frac{b}{6f^2} [b^2 + 4d^2]$$

$$T_{15,8} = \frac{b^2c}{2g^2} + \frac{b^2d}{2f^2}$$

$$T_{15,9} = \frac{d^2}{f^2} - \frac{c^2}{g^2}$$

$$T_{16,1} = -\frac{3bc^4}{10a^2g^2}$$

$$T_{16,2} = \frac{2a}{15} + \frac{c^3}{30a^2g^2} [5b^2 - 4c^2]$$

$$T_{16,3} = -\frac{3}{5} + \frac{3c^4}{5a^2g^2}$$

$$T_{16,4} = \frac{bd}{10a^2f^2} [10acd + 3d^3]$$

$$T_{16,5} = -\frac{a}{5} + \frac{d}{30a^2f^2} [30b^2c^2 + 40b^2cd + 15b^2d^2 + 10cd^3 + 6d^4]$$

$$T_{16,6} = -\frac{2}{5} + \frac{1}{5a^2f^2} [-5c^2d^2 + 10b^2cd + 5b^2d^2 + 5b^2c^2 + 2d^4]$$

$$T_{16,7} = -\frac{3bc^4}{10a^2g^2} + \frac{bd}{10a^2f^2} [10c^2d + 10cd^2 + 3d^3]$$

$$T_{16,8} = \frac{c^3}{10a^2g^2} [5b^2 + 2c^2] + \frac{d}{30a^2f^2} [30b^2c^2 + 20b^2cd + 5b^2d^2 - 10cd^3 - 4d^4]$$

$$T_{16,9} = \frac{c^2}{5a^2g^2} [5b^2 + 2c^2] + \frac{1}{5a^2f^2} [5c^2d^2 + 10cd^3 - 5b^2c^2 + 3d^4]$$

$$T_{17,1} = \frac{b}{30g^2} [4b^2 - 5c^2]$$

$$T_{17,2} = \frac{3b^2c}{10g^2}$$

$$T_{17,3} = -\frac{3b^2}{5g^2}$$

$$T_{17,4} = \frac{b}{30f^2} [5d^2 - 4b^2]$$

$$T_{17,5} = \frac{3b^2d}{10f^2}$$

$$T_{17,6} = \frac{3b^2}{5f^2}$$

$$T_{17,7} = \frac{b}{10g^2} [-2b^2 - 5c^2] + \frac{b}{30f^2} [6b^2 + 15d^2]$$

$$T_{17,8} = \frac{3b^2c}{10g^2} + \frac{3b^2d}{10f^2}$$

$$T_{17,9} = \frac{1}{5g^2} [-2b^2 - 5c^2] + \frac{1}{5f^2} [2b^2 + 5d^2]$$

APPENDIX B

COMPUTER ANALYSIS

A computer program was written in FORTRAN IV language for the IBM 7040 digital computer for a complete analysis of the shell. All of the matrix algebra was performed by the use of the Scientific Subroutine Package (SSP) as provided by IBM. Due to the limited capacity of core storage, it was necessary to write the program in three phases. Output from the first two phases was recorded on tapes and read into the final phase of the program. A macro flow diagram is given in Figure B-1 to illustrate the basic steps in the solution of a shell.

The program requires the use of two data tapes, one for recording elemental properties and structural stiffness and the other for recording deformations. All node point deformations are determined at the end of Phase II while Phase III calculates the internal actions.

In the flow diagram, ELE is used to represent the elastic constants, number of elements, number of nodes, node identification, element geometry, $[\Psi]$, $[H_p]$, $[T_p]$, $[H_b]$, $[T_b]$ and $[K^0]$.

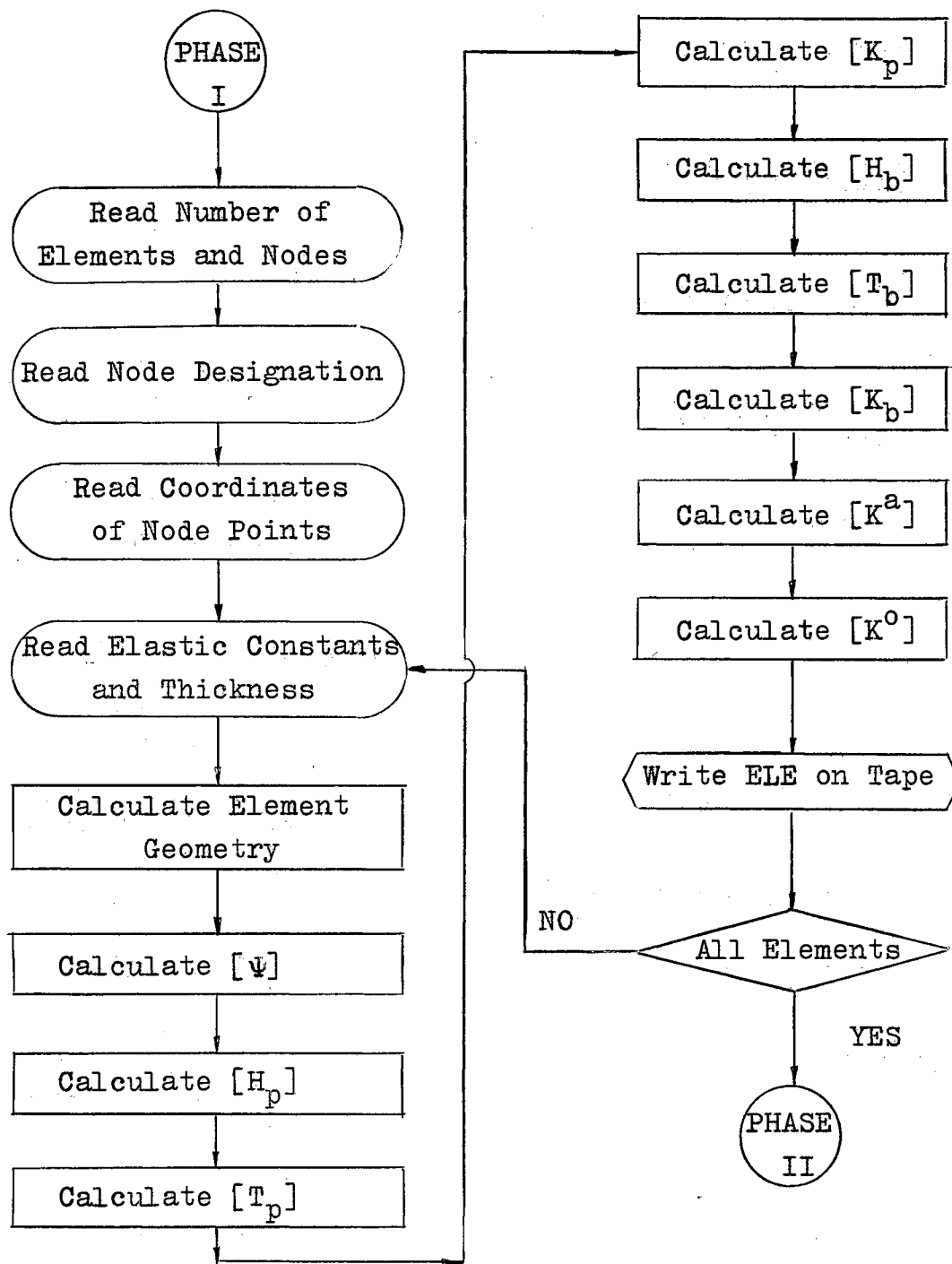


Figure B-1. Computer Flow Diagram

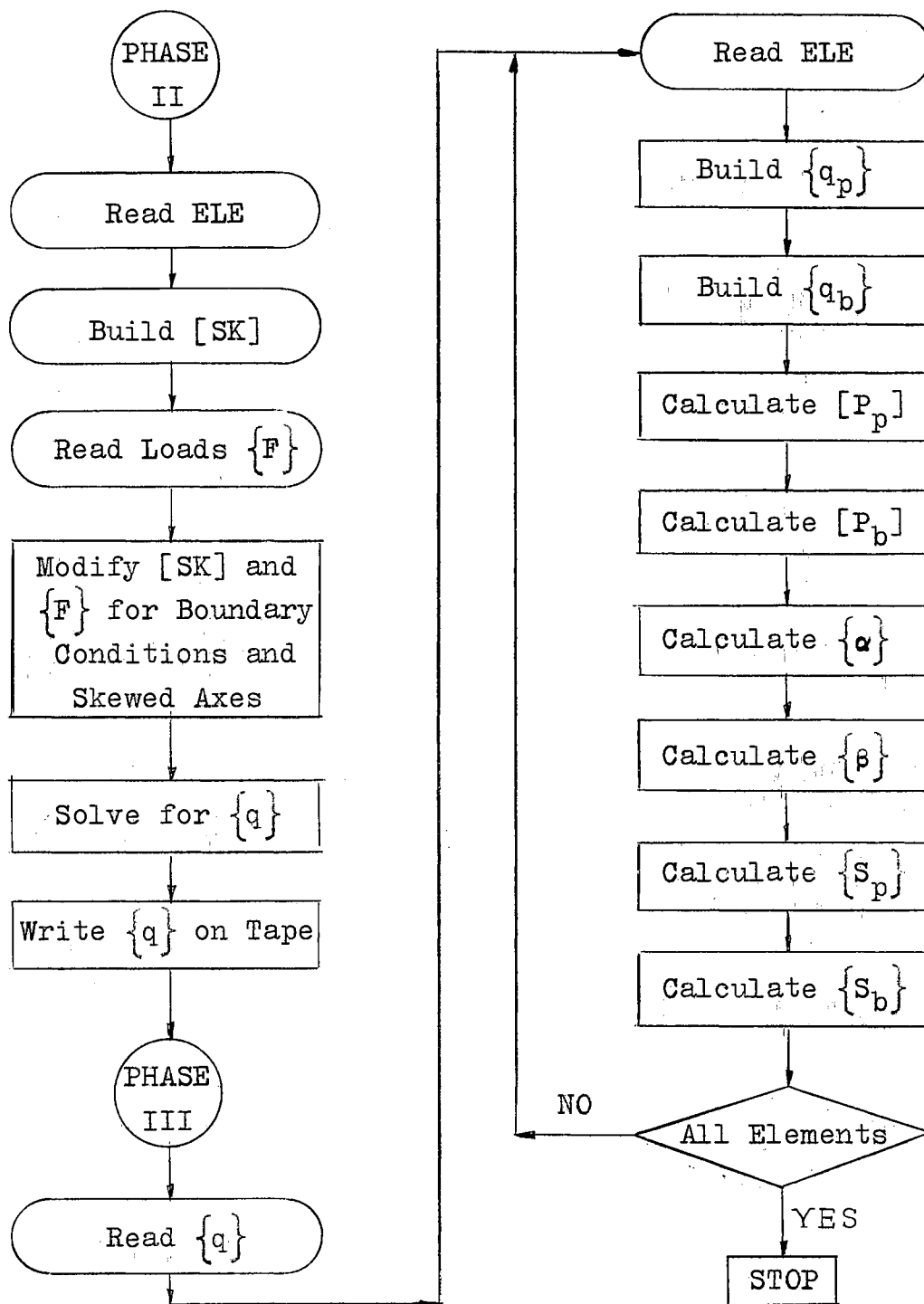


Figure B-1. Concluded

VITA

Ronald Anthony Apanian

Candidate for the Degree of
Doctor of Philosophy

Thesis: FRAME ANALYSIS OF THIN SHELLS

Major Field: Civil Engineering

Biographical:

Personal Data: Born at Bottineau, North Dakota,
October 17, 1934, the son of Anthony and Carla
Apanian.

Education: Attended grade school at Souris, North
Dakota; graduated from Souris High School in 1952;
received the Bachelor of Science degree from the
University of North Dakota, at Grand Forks, with
a major in Civil Engineering, in June, 1956;
received the Master of Science degree from the
University of North Dakota, at Grand Forks, with
a major in Civil Engineering, in June, 1958;
completed requirements for the Doctor of Philosophy
degree in May, 1967.

Professional experience: Graduate Assistant in the
school of Civil Engineering, University of North
Dakota, 1956-1957. Instructor and Assistant
Professor in the school of Civil Engineering,
University of North Dakota, 1957-1966. Design
Engineer for I. R. Jensen, R. P. E., 1956-1958.
Design Engineer with L. W. Burdick, Consulting
Firm, 1958-1965. Member of National Society of
Professional Engineers, North Dakota Society of
Professional Engineers, Associate Member of
American Society of Civil Engineers. Registered
Professional Engineer in the state of North Dakota.